U.S. Geological Survey
Open-File Report 02-412

Abstracts of the Annual Meeting of Planetary Geologic Mappers

June 21–22, 2002
Tempe, Arizona

Tracy K.P. Gregg,[1] Kenneth L. Tanaka,[2] and David A. Senske,[3]
Editors

[1]Department of Geology, University at Buffalo, Buffalo, N.Y.
[2]U.S. Geological Survey, Astrogeology Team, Flagstaff, Ariz.
[3]National Aeronautics and Space Administration, Washington, D.C.

INTRODUCTION

The annual meeting of planetary geologic mappers allows mappers the opportunity to exchange ideas, experiences, victories, and problems. In addition, presentations are reviewed by the Geologic Mapping Subcommittee (GEMS) to provide input to the Planetary Geology and Geophysics Mapping Program review panel's consideration of new proposals and progress reports that include mapping tasks. Funded mappers bring both oral presentation materials (slides or viewgraphs) and map products to post for review by GEMS and fellow mappers. Additionally, the annual meetings typically feature optional field trips that offer Earth analogs and parallels to planetary mapping problems or workshops that provide information and status of current missions.

The 2002 meeting of planetary geologic mappers was held June 21-22 at the Mars Flight Facility, Arizona State University, Tempe, Arizona. Dr. Phil Christensen graciously offered the use of the newly renovated facility, and Ms. Kelly Bender not only proved to be a courteous hostess, but also arranged a short workshop on June 23 regarding TES and THEMIS data.

Approximately 30 people attended each day of the 2-day meeting, although not the same 30—some attended only on Thursday and others only on Friday. On Thursday, eight mappers gave oral presentations of Mars mapping, and an additional two presentations were presented as posters only. Eight oral presentations on Venus mapping were given on Friday, and an additional four presentations were posters only. Twelve people attended the TES/THEMIS workshop. Presentations of Ganymede mapping and Europa mapping (the latter not yet financially sponsored by PG&G mapping program) were also given on Friday. Aside from the regular presentations of maps-in-progress, there were some additional talks. Lisa Gaddis (USGS) presented a proposal seeking support for a new lunar mapping program in light of all the new data available; she made a good case that the GEMS panel discussed. Jim Skinner (USGS) gave a short presentation on free (or nearly so) software available for 3D viewing of planetary surfaces.

Healthy discussions focused on the review time for some maps and the use of different styles of correlation charts observed on the presented maps. Next year's meeting will be held June 19-20 at Brown University, Providence, RI.

Download the abstracts as a PDF document

Download a copy of Acrobat Reader version 5.0 for free

CONTENTS

Mars

Venus

Galilean satellites

Moon

GEOLOGIC MAP OF THE MTM 85080 QUADRANGLE, PLANUM BOREUM REGION OF MARS

K.E. Herkenhoff, U. S. Geological Survey, 2255 N. Gemini Dr., Flagstaff, AZ 86001 (kherkenhoff@usgs.gov).

Introduction. The polar deposits on Mars probably record martian climate history over the last 10^7 to 10^9 years [1]. The area shown on this 1:500,000-scale map includes polar layered deposits and polar ice, as well as some exposures of older terrain. This quadrangle was mapped in order to study the relations among erosional and depositional processes on the north polar layered deposits and to compare them with the results of previous 1:500,000-scale mapping of the south polar layered deposits [2,3].

The polar ice cap, areas of partial frost cover, the layered deposits, and two nonvolatile surface units—the dust mantle and the dark material—were mapped in the south polar region [4] at 1:2,000,000 scale using a color mosaic of Viking Orbiter images. We constructed Viking Orbiter rev 726, 768, and 771 color mosaics (taken during the northern summer of 1978; fig. 1) and used them to identify similar color/albedo units in the north polar region, including the dark, saltating material that appears to have sources within the layered deposits [5]. However, no dark material has been recognized in this map area. There is no significant difference in color between the layered deposits and the mantle material mapped by Dial and Dohm [6], indicating that they are either composed of the same materials or are both covered by eolian debris [3,4]. Therefore, in this map area the color mosaics are most useful for identifying areas of partial frost cover. Because the resolution of the color mosaics is not sufficient to map the color/albedo units in detail at 1:500,000 scale, contacts between them were recognized and mapped using higher resolution black-and-white Viking Orbiter images.

No craters have been found in the north polar layered deposits or polar ice cap [7,8]. The observed lack of craters larger than 300 m implies that the surfaces of these units are no more than 100,000 years old or that they have been resurfaced at a rate of at least 2.3 mm/yr [8]. The recent cratering flux on Mars is poorly constrained, so inferred resurfacing rates and ages of surface units are uncertain by at least a factor of 2.

Stratigraphy and structure. The oldest mapped unit, mantle material (unit Am), is distinguished by its rough, sometimes knobby surface texture. The knobs and mesas of mantle material that crop out within areas of smooth layered deposits suggest that the mantle material was partly eroded before the layered deposits were laid down over them. The layered deposits appear to cover the mantle material except on steep scarps that expose the mantle material. The layered deposits may be more resistant to erosion than the mantle material, so that the steep scarps formed by more rapid erosion of mantle material beneath layered deposits. Therefore, the mantle material in this area does not appear to have been derived from erosion of the polar layered deposits.

The layered deposits (unit Al) are recognized by their distinct bedded appearance, red color, and lower albedo relative to the polar ice cap and frost deposits; they appear to be the youngest bedrock unit in this area. In both polar regions, layers are apparent at least partly because of their terraced topography, especially where accented by differential frost retention [13,14]. MOC images show that layered deposit exposures are commonly rough, with evidence for deformed beds and unconformities [16]. No definite angular unconformities have been found within the south polar layered deposits [2,3], unlike the north polar layered deposits, where truncated layers have been recognized in higher resolution images [7,13]. Angular unconformities have been found in various locations within this map

area, including lat 85.7° N., long 61° W., lat 82.6° N., long 82° W., and lat 83.6° N., long 90° W. The unconformities are mapped using hachures on the side of the contact where layers are truncated. The final line color and symbol to be used to map such unconformities will be decided during the production of this map.

The partial frost cover (unit Af) is interpreted as a mixture of seasonal frost and defrosted ground on the basis of its albedo, color, and temporal variability. Bass and others [17] found that frost albedo reaches a minimum early in the northern summer and then *increases* during the rest of the summer season. This behavior is illustrated in figure 1, where frost appears darker because it is less red. The increase in albedo is interpreted as resulting from condensation of H_2O from the atmosphere onto cold traps in the north polar region [17]. Because the images used for the base and for mapping were taken in mid-summer, the extent of the high-albedo units shown on this map is greater than during early summer.

The albedo of the residual polar ice cap (unit Ac) is higher than all other units on this map. The contact with the partial frost cover (unit Af) is gradational in many areas, most likely because unit Af represents incomplete cover of the same material (H_2O frost) that comprises unit Ac. The summer extent of the north polar cap was the same during the Mariner 9 and Viking Missions [17], which suggests that it is controlled by underlying topography. Albedo patterns in these summertime images are correlated with topographic features seen in springtime images. Areas of the highest albedoes must be covered by nearly pure coarse-grained ice or dusty fine-grained frost [18,19]. The presence of perennial frost is thought to aid in the long-term retention of dust deposits [20], so areas covered by frost all year are the most likely sites of layered-deposit formation.

The MTM 85080 geologic map has been reviewed and accepted for publication in the USGS Geologic Investigations Series. Unfortunately, map production has been delayed because the linework was completed on an old version of the Viking MDIM photomosaic base. The offset between the old and new (MDIM 2.0) base is significant, so that the linework must be shifted manually. This process is time-consuming, but publication is expected early in 2003.

References. [1] Thomas P. and others (1992) Polar deposits on Mars, in Mars, University of Arizona Press, 767-795. [2] Herkenhoff K.E. and Murray B.C. (1992) USGS Misc. Inv. Series Map I-2304; Herkenhoff K.E. and Murray B.C. (1994) USGS Misc. Inv. Series Map I-2391; Herkenhoff K.E. (2001) USGS Misc. Inv. Series Map I-2686. [3] Herkenhoff K.E. (1998) USGS Misc. Inv. Series Map I-2595. [4] Herkenhoff K.E., and Murray B.C. (1990) JGR, 95, 1343-1358. [5] Thomas P.C. and Weitz C. (1989) Icarus, 81, 185-215. [6] Dial A.L. Jr. and Dohm J.M. (1994) USGS Misc. Inv. Series Map I-2357. [7] Cutts J.A. and others (1976) Science, 194, 1329-1337. [8] Herkenhoff K.E. and Plaut J.J. (2000) Icarus, 144, 243-253. [9] Zuber M.T. and others (1998) Science, 282, 2053-2060. [10] Smith D.E. and others (1999) Science, 284, 1495-1503. [11] Murray B.C. and others (1972) Icarus, 17, 328-345. [12] Cutts J.A. (1973) JGR, 78, 4231-4249. [13] Howard A.D. and others (1982) Icarus, 50, 161-215. [14] Herkenhoff K.E. and Murray B.C. (1990) JGR, 95, 14,511-14,529. [15] Blasius K.R. and others (1982) Icarus, 50, 140-160. [16] Edgett K.S. and Malin M.C. (1999) LPS XXX, Abstract #1029; Malin M.C. and Edgett K.S. (2001) JGR, 106, 23,429-23,570. [17] Bass D.S. and others. (2000) Icarus, 144, 382. [18] Clark R.N. and Lucey P.G. (1984) JGR, 89, 6341-6348. [19] Kieffer H.H. (1990) JGR, 95, 1481-1493. [20] James P.B. and others (1979) Icarus, 68, 422-461.

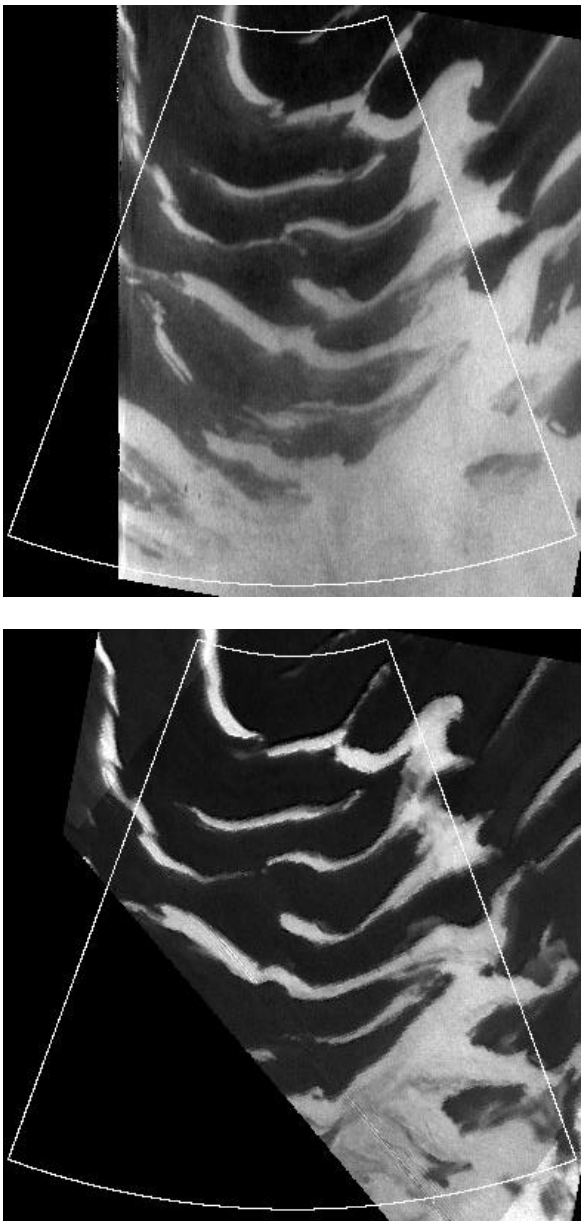

Figure 1. Red/violet ratio mosaics of Viking Orbiter 1 images of the map area, taken almost a Mars year after the images used to create the photomosaic base map. White corresponds to red/violet = 2.2, totally black regions indicate no image coverage or red/violet < 1.5. Polar stereographic projection (same as map base; map outline shown), north is up. Area shown in each mosaic ~310 km across. (top) Rev 726 mosaic (L_s = 100°), taken during a period of hazy atmospheric conditions. (bottom) Rev 768 mosaic (L_s = 119°), showing much clearer atmospheric conditions and changes in frost distribution.

GEOLOGIC MAPPING OF THE NORTHERN PLAINS OF MARS: LATEST RESULTS

K.L. Tanaka, J.A. Skinner, T.M. Hare, T. Joyal, and A. Wenker. U.S. Geological Survey, 2255 N. Gemini Dr., Flagstaff, AZ 86001, USA; ktanaka@usgs.gov.

Introduction. Geologic mapping of the northern plains of Mars, based on Mars Orbiter Laser Altimeter (MOLA) topography and Viking and Mars Orbiter Camera (MOC) images, reveals new insights into geologic and climatic events in this region during the Hesperian and Amazonian Periods. Major erosional features along the highland/ lowland boundary (HLB) indicate degradation of highland material and transport of clastic debris into the northern plains; in turn, the plains are marked by a variety of landforms indicating complex modification. Here, we offer stratigraphic revisions for the materials of the northern plains. Our observations and interpretations point to three major lowland resurfacing events during the Early Hesperian, Late Hesperian, and Late Hesperian/Early Amazonian and subsequent localized, resurfacing through similar processes. These events obliterated most preexisting morphologic and stratigraphic signatures. Based on these results, we interpret that northern plains modification was dominated by in situ, volatile-driven processes, whereas transport and deposition of highland detritus via outflow channels played a lesser role. We also do not find strong evidence for a former northern plains-filling ocean.

Stratigraphy. We identify 23 units associated with the resurfacing of the northern plains using integrated Viking Orbiter and Mars Global Surveyor data sets. The following discussion only partly describes our mapped units, highlighting the key observations and interpretations of our study thus far.

The knobby unit forms much of the highland margin, particularly along northern Arabia Terra and southern Utopia Planitia and consists of knobs and mesas of highland rocks with intervening slope and plains materials. This unit includes broad, confined depressions and low terraces. Interpretation: Fractured and collapsed highland rocks and detritus due to sapping and mass wasting of HLB subsurface volatile reservoirs. The unit reflects erosion extending from the end of the Noachian into the Early Hesperian [1-3].

The HLB is composed of plains materials that encircle most of the northern plains. Boundary plains unit 1 occurs adjacent to older highland materials including the knobby unit along the HLB in Utopia, Chryse, Amazonis, and Arcadia Planitiae. The unit's surface slopes gently away from the highland margin and is marked by irregular depressions and scarps many ten's of kilometers across and 200-300 m in relief, giving the unit a broadly scalloped appearance. Several "ghost craters" occur within the unit, forming shallow (<200 m) circular depressions with low (few tens of meters high), discontinuous rims. Boundary plains unit 2 forms a smooth surface abutting the rugged base of boundary plains unit 1 in Utopia, Chryse, and Arabia. Elsewhere, the unit embays highland material (Acidalia Planitia, Tempe Terra, and fretted terrain of northern Arabia) and older lobate material (Amazonis Planitia). Interpretation: Boundary plains units 1 and 2 likely record two successive stages of HLB degradation. The materials' morphology, elevation, and location suggest that they formed through widespread periods of mass wasting of highland rocks, erosional detritus, and local volcanic materials by volatile-driven collapse, comminution, transport, and deposition. Boundary plains unit 1 formation coincides with that of the knobby unit.

Older lobate material consists of tongue-shaped flows and forms the gently sloping shields of the Elysium and Tharsis rises and Syrtis Major Planum. Interpretation: Early Hesperian to Early Amazonian lava flows and other possible interlayered volcanic rocks.

The Scandia unit forms discontinuous plateaus and knobs within Scandia Colles.

Some northern occurrences of the unit are disrupted by depressions lined with younger chaos material. Interpretation: Severe modification of the unit inhibits the confident determination of its relative age and formational process. We interpret it to have formed during the Hesperian, possibly as highly friable, fine-grained deposits derived from eroded highland rocks or reworked pyroclastic material.

Materials related to Chryse outflow channel activity include channeled plains material and older chaos material. Channeled plains material covers the floors of the broad Chryse outflow channels; its northern extent is disrupted by the Vastitas Borealis Formation (VBF). The spatially and temporally related older chaos material forms irregular depressions tens to hundreds of kilometers across and hundreds of meters to more than a kilometer deep south of Chryse Planitia. These depressions are filled with irregular knobs and fractured mesas and form the apparent source regions for the Chryse outflow channels. Interpretation: Disrupted and eroded highland material subjected to collapse and comminution within chaos depressions due to explosive volatile discharge, perhaps related to volcanic activity, and deposited in channel floors by fluvial transport and/or mass flow.

The Vastitas Borealis Formation covers the majority of the Borealis, Utopia, and Isidis basin floors. Though previous maps divide the VBF into grooved, ridged, mottled, and knobby members, our observations suggest these divisions reflect differences in surface modification rather than distinctions in lithology, origin, or age. Because the more widespread, subtler morphologies that characterize the VBF are commonly more apparent in high-resolution (~500 m) MOLA DEM's than Viking Orbiter images, we are able to more accurately map and characterize the VBF contact. We divide the VBF into a regional hummocky member and a local marginal member. The hummocky member is marked by numerous low hillocks and arcuate ridges (in places organized into thumbprint terrain), patches of polygonal grooves, local systems of mostly asymmetric, low ridges, dozens of circular depressions ("ghost craters") up to tens of kilometers in diameter, and by many superposed, relatively high albedo, mostly rampart and some pedestal craters. The marginal member forms low plateaus with rounded margins and linear to sinuous troughs, many of which terminate at or connect to large knobs. Interpretation: We interpret the VBF as a mélange of Noachian to Hesperian materials [6-7], including remnants of highland rocks, mass-wasting detritus, outflow-channel deposits, and volcanic plains that have been highly and pervasively altered by in situ volatile-driven processes. These processes may include cryoturbation, desiccation, thermokarst, and local mass-movements aided by subsurface volatiles. Though the unit has an overall end-of-the-Late-Hesperian crater density [1], its formation could well have extended into the Early Amazonian based on variable local distributions of craters.

Younger chaos material occurs within depressions tens to hundreds of kilometers across and tens to a few hundreds of meters deep in the Acidalia, Cydonia, and Scandia regions. The unit locally includes polygonal fractures, knobs, and irregular scarps. Some patches of low-lying and particularly smooth chaos in southern Chryse Planitia may reflect younger chaos material formed after widespread development of the outflow channels. Interpretation: VBF and channel materials that have been disrupted and eroded by volatile discharge and subsequent collapse.

The tholi unit forms circular to irregular domical hills and rugged complexes tens to a few hundred kilometers across and tens to hundreds of meters high in the Scandia region. The larger complexes have interior depressions tens to hundreds of meters deep and a few narrow sinuous ridges a couple kilometers wide and tens of kilometers long. Many of the hills are bounded by shallow moats. Interpretation: Lava, mud, or ice extrusions formed the

domes and perhaps phreatic or cryoclastic eruptions and discharge-related collapse produced the depressions and moats.

Coarse lobate material occurs in Amazonis and Utopia Planitiae, often in temporal and spatial association with smooth lobate material. These materials, which emanate from various fissures along the northwestern and southeastern flanks of the Elysium rise, include diverse hummocky, pitted, and channeled surfaces that embay and dissect large ejecta blankets. Interpretation: Amazonian hydrovolcanic debris floods of variable lithic and volatile components formed by both extrusive and mass-wasting processes.

Smooth lobate material (2 units) consists of tongue-shaped flows tens of kilometers wide and hundreds of kilometers long in Amazonis and Utopia Planitiae. Interpretation: Amazonian lava flows produced from highly effusive eruptions.

The lower polar layered deposits (LPLD) form the base of Planum Boreum and possibly high-standing knobs and mesas south of Chasma Boreale and underlie the evenly bedded polar layered deposits. The unit's texture resembles that marking the adjacent VBF and may be indicative of similar modification. The unit's thickness of >1 km (as observed in Chasma Boreale) thins toward the margins of the polar layered deposits. MOC images and MOLA data reveals irregular bedding, locally steep scarps, and a dark color within the LPLD. Interpretation: Possibly an eroded sand sea [10] or modified polar layered deposits. Both the Scandia unit and LPLD may represent remnants of a single expansive deposit. LPLD was likely much more continuous, perhaps accounting for the occurrence of pedestal craters in the plains surrounding Planum Boreum.

Later polar resurfacing includes deposition of upper polar layered deposits and residual polar ice on top of Planum Boreum and deposition of hummocky and dune materials in the plains surrounding the planum.

Future work. We hope to complete our geologic map of the northern plains of Mars by the end of 2002. Further mapping tasks include subdivision of ancient highland rocks and volcanic units ~300 km inward from the highland margin, which will provide context for compositional information obtained by Mars Global Surveyor's TES mineralogic and Mars Odyssey's GRS elemental and THEMIS thermal properties data. Such data may assist in testing hypotheses for the origin, provenance, and modification histories of lowland units relative to possible highland source rocks as indicated by our mapping.

References. [1] Tanaka K.L. (1986) JGR, 91, E139-E158. [2] Scott D.H. et al. (1986-87) USGS Map I-1802-A, B, C. [3] Maxwell, T.A. and McGill G.E. (1987) PLPS, 18, 701–711. [4] Tanaka, K.L. (1997) JGR, 102, 4131-4149. [5] Parker, T.J. et al. (1989) Icarus, 82, 111-145. [6] Kreslvasky M.A. and Head J.W. III (2001) LPSC Abs. #1001. [7] Frey H. et al. (2001) GRL, in press. [8] Carr, M.H. and Schaber G.G. (1977) JGR, 82, 4039-4053. [9] Fishbaugh K.E. and Head J.W. III (2000) JGR, 105, 22455-22486. [10] Murray B.C. et al. (2001) Eos Trans. AGU, 82, F694. [11] Smith D.E. et al. (2001) Science, 284, 1495-1503. [12] Tanaka K.L. et al. (1991) JGR, 95, 15617-15633. [13] Thomson B.J. and Head J.W. III (2001) JGR, 106, 23209-23230. [14] Christensen P.R. et al. (2001) JGR, 106, 23823-23871.

GEOLOGIC MAPPING OF THE MARTIAN HIGHLANDS: TERRA TYRRHENA AND PROMETHEI TERRA

David A. Crown[1] and Scott C. Mest[2], [1]Planetary Science Institute, 620 N. 6th Avenue, Tucson, AZ 85705, [2]Department of Geology and Planetary Science, University of Pittsburgh, Pittsburgh, PA 15260, crown@psi.edu and scmst25+@pitt.edu

Introduction. Geologic mapping studies and geomorphic analyses are being used to characterize ancient cratered highland terrains surrounding the Hellas basin in the southern hemisphere of Mars. General scientific objectives include identifying sequences and styles of highland degradation, determining erosional and depositional histories, and providing constraints on volatile inventories and potential climate change. The spatial and temporal variability of highland evolution is being evaluated by comparison of mapping results in different regions. Currently two MTM quadrangles (-20272 and –25272) in Terra Tyrrhena [1] and three MTM quadrangles (-35237, -40237, and –45237) in eastern Promethei Terra [2] are being mapped. The Terra Tyrrhena map area includes a large valley network dissecting cratered highlands north of the Hellas basin, and the eastern Promethei Terra map area includes large expanses of ridged plains (southeastern Hesperia Planum) and knobby plains adjacent to cratered highlands.

The current studies build on analyses of the geology of Reull Vallis region, which have included both regional and MTM mapping projects [3-6], as well as complement earlier investigations of the eastern Hellas region of Mars [7-9], volcanic studies of Hadriaca and Tyrrhena Paterae [10-13], and mapping of highland outflow channels [14]. Mapping in the Terra Tyrrhena and Promethei Terra regions is designed to provide new constraints on the styles and timing of volcanic, tectonic, mass-wasting, fluvial, and potential lacustrine processes that have contributed to the complex geologic record preserved in the circum-Hellas highlands. Current versions of maps of MTM -40252, -40257, -45252, and -45257 quadrangles (Reull Vallis region) and MTM –20272 and –25272 quadrangles (Terra Tyrrhena region) are available at http://viking.eps.pitt.edu/public/maps/maplinks.html.

Geologic Mapping of Terra Tyrrhena. Within Terra Tyrrhena, MTM -20272 and -25272 quadrangles (17.5-27.5° S., 270-275° W.) contain an extensive (~400 km long) dendritic valley network system that dissects a cratered highland surface and loses definition near a low-lying, more lightly cratered expanse of plains. Additional smaller valley networks are found on the cratered plateau and adjacent to crater Millochau, whose floor contains a partially eroded deposit with terraced hills. Key scientific issues for MTM -20272 and -25272 quadrangles include (a) characterization and potential subdivision of the dissected plateau north of Hellas to foster detailed stratigraphic comparisons around the basin, (b) descriptive and quantitative analyses of fluvial systems, and (c) documentation of crater morphologies and effects of erosion and infilling, including identification of potential lacustrine environments.

A preliminary geologic map of –20272 and –25272 quadrangles, showing the distribution of geologic units and structural features, has been completed along with compilation of crater-size frequency distributions for the major units. Geologic units mapped include: talus material, channel floor material, smooth plateau unit, dissected intercrater plains material, mountainous material, and crater materials. Mapped structural features include scarps, ridges, channels, and crater rim crests. The majority of the map area consists of dissected intercrater plains and ejecta, floor, and rim materials of the numerous, large impact craters that exhibit a wide range of preservation states. In MOC images,

dissected intercrater plains exhibit a highly degraded surface with dark albedo material filling small craters and pits. Variations in the degree of infilling are evident, with the southern part of the plains dominated by extensive dune fields. Channel floor material defines the main valley segments of the large network system that extends throughout the region. Smaller channels are found as tributaries of this large system and form small valley networks within the intercrater plains. Small, roughly parallel gullies dissect crater rim materials. Cross-cutting relationships between valleys and the abundant highland craters observed in the area, coupled with variations in crater and valley morphology, suggest a complex history of fluvial activity over a significant period of martian history.

Geologic Mapping of Promethei Terra. MTM -35237, -40237, and -45237 quadrangles (32.5-47.5° S., 235-240° W.) include part of Promethei Terra to the east of the previously studied Reull Vallis region. This area contains the ridged plains of Hesperia Planum, cratered plateau and highland regions, and knobby plains that appear to be the remnant of an older extensive plains unit. Key scientific issues for MTM -35237, -40237, and -45237 quadrangles include (a) the origin and modification of ridged plains, including documentation of sedimentary contributions, (b) evaluation of the ridged plains as a stratigraphic referent, (c) the resurfacing and erosional history of cratered terrains, and (d) the stratigraphic position and origin of the knobby plains, with specific comparisons to large depositional events adjacent to Reull Vallis.

A preliminary map of structural features (scarps, ridges, channels, and crater rim crests) for–35237, -40237, and –45237 quadrangles has been generated, and the major geologic units of the map area have been identified and characterized. Geologic units include: highland materials (mountainous material, cratered-plateau unit, basin-rim unit), ridged plains material, knobby plains material, crater materials, and surficial materials (crater fill material, debris apron material, and dune field material). The highland regions contain numerous large impact craters, some with prominent rims, well-defined ejecta blankets, and rugged floors and others with extensively degraded, low-relief forms with gullied rims and filled interiors. Intercrater regions exhibit small channels and gullies. Lobate debris aprons extend from some highland massifs.

Large expanses of ridged and knobby plains cover low-lying regions adjacent to the highlands. Ridged plains exhibit orthogonal ridge trends as well as numerous ridge rings. Within the ridged plains, rampart craters, smooth and pitted surfaces, and several long channels are observed, and scarps indicative of flow margins are evident. Knobby plains are more extensive than mapped previously by Greeley and Guest [15]. Knobs occur in clusters, some of which exhibit linear to curvilinear patterns, and within certain regions, knob spacing increases locally toward the edge of an exposure. A gradational contact with the ridged plains is apparent, and knobby surfaces are found superposed on ridged plains, within crater ejecta, and in crater interiors. Knobby plains are concentrated in low areas but are not found in all low-lying regions of the quadrangles. There is no clear evidence of deposition of any of the material that originally may have separated knobs. A complex local stratigraphy is suggested by relationships between knobs, pedestal craters, and layering within the plains. Future work will include detailed analyses of knob morphology and distribution, constraints on plains thickness from crater infilling and burial, and compilation of crater size-frequency distributions.

References. [1] Mest, S.C. and D.A. Crown, Geologic map of MTM -20272 and -25272 quadrangles, U.S. Geological Survey, in preparation, 2002. [2] Crown, D.A. and S.C. Mest, Geologic map of MTM -35237, -40237, and -45237 quadrangles, U.S. Geological Survey, in preparation,

2002. [3] Mest, S.C. and D.A. Crown, Geologic history of the Reull Vallis region, Mars, Icarus, 153, 2001. [4] Mest, S.C. and D.A. Crown, Geologic map of MTM -40252 and -40257 quadrangles, Reull Vallis region of Mars, U.S. Geological Survey Geologic Investigations Series Map I-2730, in press, 2002. [5] Mest, S.C. and D.A. Crown, Geologic map of MTM -45252 and -45257 quadrangles, Reull Vallis region of Mars, U.S. Geological Survey Geologic Investigations Series Map I-2763, in press, 2003. [6] Crown, D.A. and S.C. Mest, Geologic map of MTM -30247, -35247, and -40247 quadrangles, Reull Vallis region of Mars, U.S. Geological Survey, in preparation, 2002. [7] Crown, D.A. and others, Icarus, 100, 1-25, 1992. [8] Tanaka, K.L. and G.J. Leonard, J. Geophys. Res., 100, 5407-5432, 1995. [9] Mest, S.C., Geologic history of the Reull Vallis region, Mars, M.S. Thesis, University of Pittsburgh, 217 pp., 1998. [10] Greeley, R. and D.A. Crown, J. Geophys. Res., 95, 7133-7149, 1990. [11] Crown, D.A. and R. Greeley, J. Geophys. Res, 98, 3431-3451. 1993. [12] Gregg, T.K.P. and others, U.S. Geol. Surv. Misc. Inv. Ser. Map I-2556, 1998. [13] Crown, D.A. and Greeley, R., Geologic map of MTM -30262 and -30267 quadrangles, Hadriaca Patera region of Mars, U.S. Geological Survey, in review, 2002. [14] Price, K.H., U.S. Geol. Surv. Misc. Inv. Ser. Map I-2557, 1998. [15] Greeley, R., and J.E. Guest, U.S. Geol. Surv. Misc. Invest. Ser. Map, I-1802B, 1987.

GEOLOGY OF THE CYDONIA MENSAE/SOUTHERN ACIDALIA PLANITIA AREA, MARS

George E. McGill, Department of Geosciences, University of Massachusetts, Amherst, MA 01003. gmcgill@geo.umass.edu

The current study involves mapping and topical studies within Cydonia Mensae and southern Acidalia Planitia, in a 10x15 degree region that includes six 1:500,000-scale quadrangles: 40007, 40012, 40017, 45007, 45012, and 45017. The region was selected for study because it includes most of the Acidalia Planitia giant polygons and because, along with quadrangles 35007 and 35012, it sits astride the dichotomy boundary in an area where this boundary appears to be transitional rather than abrupt [1]. Based on Mariner 9 data, this area was briefly considered as a possible site for a Viking lander [2]; consequently, medium resolution (~45m/pxl) images of the area were collected on several Viking orbital passes. For a significant part of the area within the six quadrangles being mapped there are very high quality medium-resolution images. However, some of the medium-resolution images were taken when the atmosphere was dusty, resulting in loss of fine detail despite the favorable pixel resolution. An unfortunate gap in medium-resolution coverage occurs along the east-west boundary between quadrangles 40007 and 40012 to the north, and 35007 and 35012 to the south. Images along this boundary have resolutions of ~100-160 m/pixel. Mapping at these resolutions may not provide much new information about the geology along the dichotomy boundary, and thus mapping of 35007 and 35012 should wait for THEMIS data.

Several issues relevant to crustal evolution in this area can be addressed by mapping the six quadrangles currently under study. These include: (1) the age and origin of the abundant, small, conelike and domelike edifices that occur in all six quadrangles but that are especially abundant in 40012; (2) the age of the material hosting the Acidalia Planitia giant polygons relative to the age of the material making up the mesas and knobs of Cydonia Mensae; (3) the relationship between putative shorelines [1,3] of an ancient ocean and material contacts mapped as part of this study; (4) the dual age of Acidalia Planitia based on visually apparent clustering of large craters and a distinct kink in the crater diameter/cumulative frequency plot despite the lack of support for plains of two distinct ages in either the topography or in mappable contacts; and (5) the significance of the topography revealed by MOLA for constraining the processes responsible for the giant polygons. None of these issues has been fully resolved, but progress has been made on all of them.

The problem of the small cones and domes was reviewed at this year's Lunar and Planetary Science Conference [4]. These features have been inferred to be pseudocraters, cinder cones, pingos, mud volcanoes, or degraded secondary craters in past papers [5,6,7,8,9,10,11]. The morphology and distribution of most of these features are not consistent with a pseudocrater model, which is the favorite among past workers. However, MOC images provide evidence for distinct morphological classes of edifices, many of which are too small to be resolved by the medium-resolution Viking images. Some are likely to be pseudocraters and some likely to be tuff rings, but other analogs cannot as yet be eliminated.

The plains material of Acidalia Planitia that hosts the giant polygons could be old and once covered by younger material now present as isolated outliers (the mesas and knobs of Cydonia Mensae [12]), or else it could be young and due to deposition adjacent to the mesas and knobs of Cydonia Mensae [13], which would be inliers in this model. An old age requires extensive erosional stripping because the plains material appears to be continuous

from Cydonia Mensae northward across Acidalia Planitia. Consequently, the old-plains model implies either (1) that the small edifices and the giant polygons formed after the erosional stripping and thus that they are much younger than the plains material, or else (2) the edifices survived the erosional stripping even though all models for their origin imply poorly consolidated or unconsolidated material, and the polygon troughs were either unmodified or uniformly modified by the erosional stripping over a very large area. A relatively young age for Acidalia plains material appears to be favored by these constraints.

Preliminary analysis suggests that the proposed shorelines in this area [1,3] commonly coincide with geologic contacts defined in the present study. However, single shorelines match different contacts along their traces. More work needs to be done to determine the impact of these observations on the shoreline hypothesis. An in-progress study by graduate student Valerie Webb using Viking, MOC, and MOLA data is addressing this issue.

The crater diameter vs. cumulative frequency plot for 341 craters >1 km in diameter on Acidalia plains in quadrangles 40017, 45007, 45012, and 45017 is strongly kinked at a diameter of about 10 km. Craters smaller than 10 km clearly define an Early Amazonian age, consistent with the result reported by Tanaka [14], whereas craters larger than 10 km suggest a poorly defined age that is probably Early Hesperian. Many of these large craters appear to be clustered to an extent not expected simply from random statistics, but neither the geology nor the topography suggests the presence of a unit distinct from surrounding plains material.

Circular graben rings within polygonal terrain are inferred to occur over buried impact crater rims. If differential compaction is involved in forming the grabens, then one would predict topographic depressions within graben rings, and an increase in the depth of these depressions with increase in ring (and thus crater) diameter. These predictions have been borne out by studies in Utopia Planitia [15,16]. The inclusion of extended mission data since March has made the Utopia results even more robust. A comparable study of graben rings in Acidalia Planitia is now underway by graduate student Debra Buczkowski.

References. [1] Parker, T.J., and others, Icarus, 82, 111-145, 1989. [2] Masursky, H., and N.L. Crabill, Science, 194, 62-68, 1976. [3] Clifford, S.M., and T.J. Parker, Icarus 154, 40-79, 2001. [4] McGill, G.E., Lunar Planet. Sci. XXXIII, abs. #1126, 2002. [5] Frey, H., and others, J. Geophys. Res., 84, 8075-8086, 1979. [6] Frey, H., and M. Jarosevich, J. Geophys. Res., 87, 9867-9879, 1982. [7] Wood, C.A., Proc. Lunar Planet. Sci. Conf., 10th, 2815-2840, 1979. [8] Lanagan, P.D., and others, Geophys. Res. Letts., 28, 2365-2367, 2001. [9] Greeley, R., and S.A. Fagents, J. Geophys. Res., 106, 20,527-20,546, 2001. [10] Carr, M., and others, J. Geophys. Res., 82, 3985-4015m 1977. [11] Tanaka, K., J. Geophys. Res., 102, 4131-4149, 1997. [12] Guest, J.E., and P.S. Butterworth, J. Geophys. Res., 82, 4111-4120, 1977. [13] Witbeck, N.E., and J.R. Underwood, Jr., U.S. Geol. Surv. Misc. Invest. Map I-1614, 1984. [14] Tanaka, K.L., J. Geophys. Res., 91, E139-E158, 1986. [15] Buczkowski, D.L., and G.E. McGill, Lunar Planet. Sci. XXXIII, abs. #1020, 2002. [16] Buczkowski, D.L., and G.E. McGill, Geophys. Res. Letts., 29(7), 10.1029/2001GL014100, 59-1-59-4, 2002.

GEOLOGY OF THE HECATES THOLUS REGION (MTM 35207 AND 35212 QUADRANGLES) OF MARS

René A. De Hon, Department of Geosciences, University of Louisiana at Monroe, Monroe, LA, 71209.

Introduction: MTM 35207 and MTM 35212 quadrangles are part of a proposal to map a strip of four quadrangle on the northern edge of the continuous lava flows of Elysium Mons. One map of this series is published, Geologic map of the Galaxias quadrangle (MTM 35217) [1]. The current mapping includes the northern half of Hecates Tholus, polygonally grooved terrain of Galaxias Chaos, and abundant scattered knobs and mesas separated by smooth plains.

The northern distal margin of Elysium Mons is marked by five distinct bands of terrain that grade northward away from the Elysium volcanic construct. These bands are (1) zone of continuous Elysium lava flows, (2) chaos or grooved terrain, (3) subdued grooved terrain, (4) knob and mesa terrain, and (5) knobby terrain. Major questions to be resolved, in addition to the stratigraphy, are concerned with the origin of the chaos; the origin of wide, shallow depressions associated with subdued terrain; and the origin of knobs and mesas.

Stratigraphy: The chief strati-graphic units are materials of Hecates Tholus, flows from Elysium Mons, materials of the chaos, knob and mesa materials, and plains-forming materials of the low-lying areas. Minor channel materials, smooth plains, and crater materials round out the exposures. Because of the low numbers of superposed craters, all materials other than a few partially buried craters and Hecates Tholus are interpreted to be Amazonian in age. Materials are mapped as four major groups: northern volcanic assemblage, northern plains assemblage, channel-system materials, and impact crater materials.

The northern volcanic assemblage consists of materials of Hecates Tholus and Elysium Mons. The oldest exposed noncrater material in the region is material of Hecates Tholus (unit Hhet), which comprises a domical rise approximately 165 km in basal diameter and 7 km high. Hecates is flanked and partially overlapped by materials of the Elysium Formation (units Ael2a and Ael2b). These are relatively fresh appearing lobate flows with low numbers of superposed craters.

The northern plains assemblage consists of rugged terrains formed by the break up of Elysium lavas (unit Apg, grooved plains material; unit Akm, knob and mesa material; unit Apk, knobby plains material; and unit Aps, intervening smooth-plains-forming materials). The grooved terrain is characterized by polygonally shaped mesas up to 20 km across, separated by 1- to 2-km-wide, flat-floored troughs. This material is interpreted as Elysium lavas broken by removal dewatering of subjacent ice-laden materials. Various origins have been proposed for the knobs and mesas. Origins proposed for these features include small volcanic constructs [2], sub-ice volcanoes [3], pingos [1, 2], and erosional remnants of a plateau surface [4, 5]. I interpret the grooved terrain, mesas, and knobs as erosional remnants (outliers) of a northward-thinning cap of Elysium flow materials. Smooth plains material forms extensive low-lying plains covering the area between knobs and mesas. Some plains material floors depressions and is probably local lacustrine or eolian material. The widespread plains material has been interpreted as lacustrine [6], marine [7], or glacial [3] in origin.

Channel-related materials: The surface of Hecates Tholus is cut by many small channels. Two prominent channels (unit Ach) 2 to 4 km wide occur near the base of Hecates Tholus. Channel flood-plain material (unit Achp) floors basins surrounded by grooved material. These

basins feed outflow channels in the adjoining Galaxias quadrangle.

Crater materials: A few partially buried craters with uncertain stratigraphic bases are designated as Amazonian or Hesperian material (unit Ahc). All other craters are assumed to be Amazonian in age as they are topographically sharp and superposed on all other materials. The largest crater is 12 km in diameter and most are less than 7.5 km in diameter. Secondary crater clusters are prominent. Most craters greater than 4 km in diameter display lobate deposits with distal ramparts characteristic of craters believed to have been formed in volatile-rich target materials.

Structure: The dominant structural trend is northwest; follows the regional slope; and is roughly radial to Elysium Mons. Features of presumed structural significance include fissures in Elysium lavas and vague lineaments in knobby terrain.

One-kilometer-wide grooves outline polygonal blocks of grooved terrain. The surfaces of the blocks are not tilted in a disordered or jumbled fashion as common to chaotic terrain. Grooves appear to be polygonal fractures widened by erosion, or perhaps, by slight displacement of competent lavas overlying a decaying ice décollement.

References: [1] De Hon, R.A., P.J. Mouginis-Mark, and E.E. Brick, 1999, *U.S. Geol. Surv. Series Misc. Inves.* Map I-2579. [2] Scott, D.H. and K.L. Tanaka, 1986, *U.S. Geol. Surv. Misc. Inves.* Map I-1802A. [3] Chapman, M.G., 1994, *Icarus 109*, 393-406. [4] Greeley, R. and J.E. Guest, 1987, *U.S. Geol. Surv. Series Misc. Inves.* Map I-1802B. [5] De Hon, R.A., 1997, *Lunar and Planetary Science XXVIII,* 289-290. [6] Scott D.H., M.G. Chapman, J.W. Rice, and J.M. Dohm, 1992, *Proc. Lunar and Planetary Science Conf., 23nd*, 53-62. [7] Baker,V.R., R.G. Strom, S.K. Croft, V.C. Kargel, and G. Komatsu, 1990, *Lunar and Planetary Science XXI,* 40-41.

GEOLOGIC MAPPING IN MARGARITIFER SINUS, MARS

J. A. Grant[1] and D.A. Clark[1], [1]Center for Earth and Planetary Studies, National Air and Space Museum, MRC 315, Smithsonian Institution, Washington, DC 20560, grantj@nasm.si.edu.

Introduction. Geologic and drainage mapping in Margaritifer Sinus [1, 2] at 1:500,000 (MTM –10022, -15022, -20012, –25012 quadrangles) incorporates results of nearby mapping efforts [3, 4] and details a complex history of water transport, storage, and release along the Chryse trough [5, 6] (fig. 1). The segmented Uzboi-Ladon-Margaritifer (ULM) northward-flowing mesoscale outflow system drains more than 11 X 10^6 km^2 or about 9% of Mars [5] and incises and fills as it crosses a series of ancient multi-ringed impact basins [6, 7] on the western flank of the trough [3, 4]. By contrast, Samara and Parana-Loire Valles, two of the best integrated valley systems on Mars [1], drain more than 540,000 km^2 (about 0.5% of Mars) on the eastern flank of the trough. Drainage was from the late Noachian into mid-Hesperian and all systems terminate in the Margaritifer basin along the trough axis near the head of Ares Vallis [2].

Geologic History of the Margaritifer Sinus Region. Geologic mapping at 1:2,000,000 and 1:500,000 [2-4] identifies the degraded Ladon and Holden multi-ringed impact basins [6, 7] as the oldest features in Margaritifer Sinus (figs. 2, 3). Basin formation was followed by evolution of the cratered upland surface and three widespread resurfacing events that deposited materials interpreted to be of mostly volcanic origin on the basis of wrinkle ridges and occasionally lobate morphology. The first two events occurred during Early Noachian heavy bombardment [9] with the second ending at an N5 age of 1400 (number of craters >5 km in diameter per 1,000,000 km^2). The third resurfacing event from the Middle to Late Noachian (N5 of 500-300) was coincident with waning highland volcanism [8].

Incisement of the ULM segments, infilling of intervening basins, cutting of Samara and Parana-Loire Valles, and incisement of all nearby valleys took place from Late Noachian into the Early Hesperian (N5 of 300-150). Channel and valley formation coincided with increased geomorphic activity elsewhere on Mars [1, 2, 9]. Discharge along the ULM system was greatest and was likely on the order of 150,000 m^3sec^{-1} and 450,000 m^3sec^{-1} [2]. Estimated discharge along ULM is 5-10 times greater than the discharge of the Mississippi River [10], but on the low end of discharge estimates for the Channeled Scabland [11-12]. A final, more localized resurfacing event occurred in the Early to middle Hesperian (N5 ages 200 to 70) and emplaced material that embays all valleys and channels.

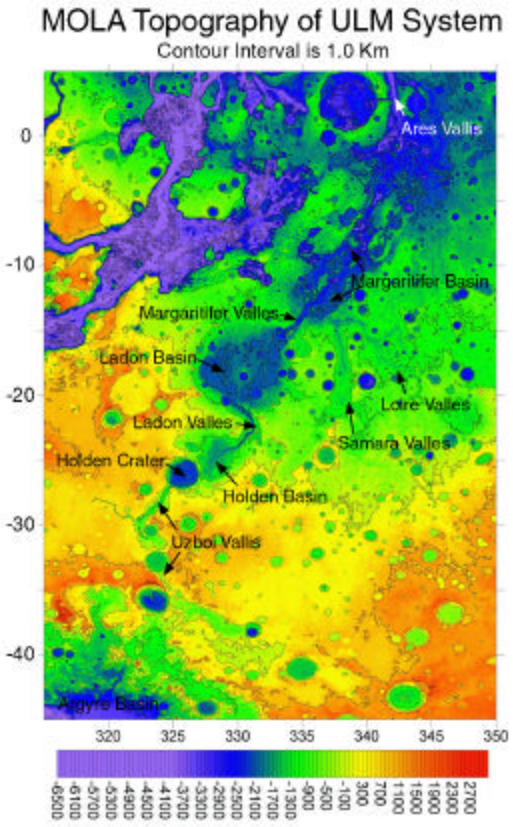

Figure 1. MOLA topography of Margaritifer Sinus region. Chryse trough axis runs through the right center of the image (reproduced from fig. 1 in [8]).

The ULM and Samara and Parana-Loire systems all discharge into Margaritifer basin, a depositional plain lying ~2 km

below the MOLA datum. Smooth plains that embay most adjacent surfaces (except those cut by chaos or buried by materials emplaced during the fourth resurfacing event) characterize the depositional floor of the basin, and the northeastern extent is indistinct due to collapse of Margaritifer and Iani Chaos. Nevertheless, the plain extends at least to the head of Ares Vallis and maybe well beyond [2]. It is likely that discharge into Margaritifer basin resulted in considerable ponding, subsurface infiltration, and storage of water [2].

Collapse within and adjacent to Margaritifer basin and formation of Margaritifer and Iani Chaos began shortly after cessation of channel and valley formation in the Early to middle Hesperian and likely re-released the stored water, thereby causing incisement of Ares Vallis. Hence, it appears that formation of Ares Vallis was the final stage in a long history of repeated water collection, transport, storage, and discharge in the Margaritifer Sinus region.

References. [1] Grant, J.A. (2000) Geology, 28, 223-226. [2] Grant, J. A., and Parker, T.J., (2002), JGR, 107 (in press). [3] Parker, T.J. (1985) Master's Thesis, California State Univ., LA, 165. [4] Parker, T.J., (1994) Ph.D. Thesis, Univ. Southern California, LA. [5] Banerdt, W. B. (2000) Eos, 81, P52C-04. [6] Saunders, S. R. (1979) USGS I-1144, USGS. [7] Schultz, P. H., et al. (1982) JGR, 87, 9803-9820. [8] Grant, J.A., and Parker, T.J. (2002) LPSC XXXIII, CD-ROM. [9] Scott, D. H. and Tanaka, K. L. (1986) USGS Misc. Inv. Series Map I-1802-A, USGS. [10] Komar, P.D. (1979) Icarus, 37, 156-181. [11] Baker, V. R. (1982) The Channels of Mars: Austin, Univ. Texas Press, 198. [12] Baker, V.R. and Nummedal, D. (1978) The Channeled Scabland: A Guide to the Geomorphology of the Columbia Basin, Washington, NASA, Washington, 186.

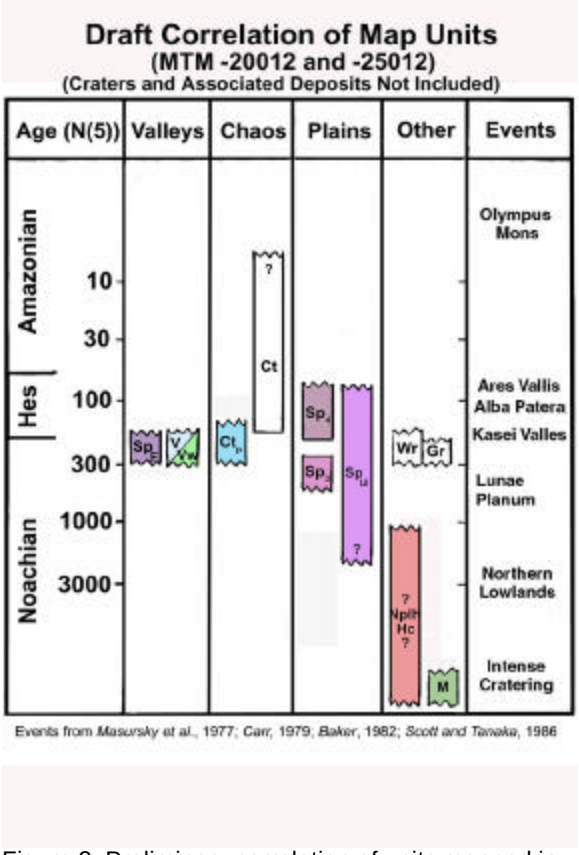

Figure 2. Preliminary correlation of units mapped in MTM–20012 and –25012 quadrangles. N5 ages and units are representative of preliminary units mapped in nearby MTM –10022 and -15022 quadrangles. Figure modified from figure 2 in [1] and figure 4 in [2] and does not yet incorporate standard symbols or colors.

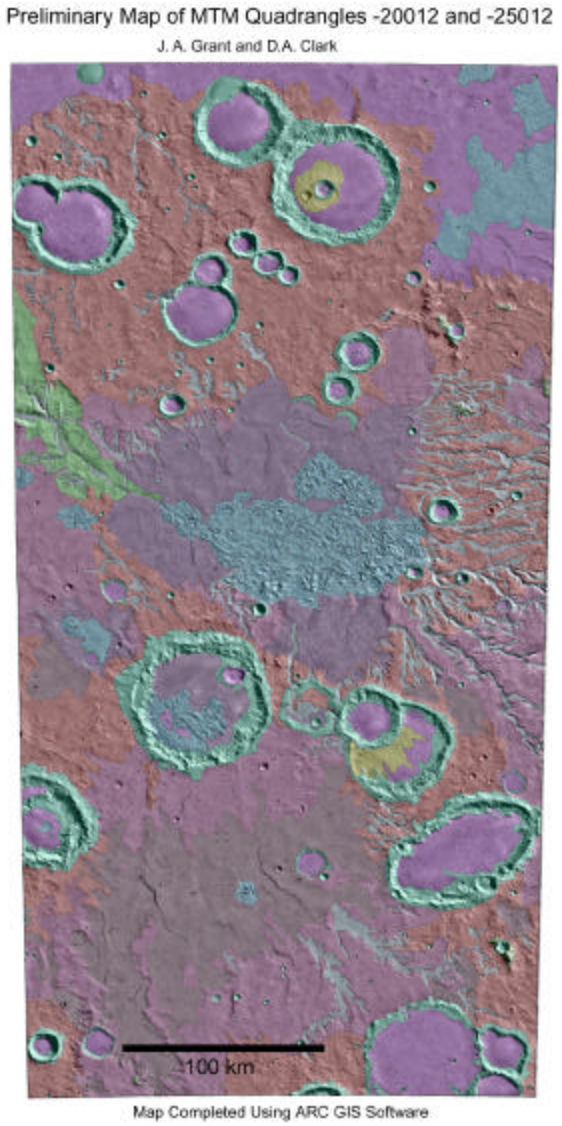

Figure 3. Preliminary map of MTM –20012 and –25012 quadrangles in Margaritifer Sinus. Region encompasses much of Parana Valles, the depositional Parana basin and other associated tributary systems, and the head of the northwestward-flowing Loire Valles. North is toward the top and preliminary explanation/correlation of units is given in fig. 2. Map does not yet incorporate standard symbols or colors.

GEOLOGIC MAPPING OF MARS (MEDUSAE FOSSAE FORMATION) AND VENUS (BELLONA FOSSAE QUADRANGLE, V-15)

James R. Zimbelman, CEPS/NASM MRC 315, Smithsonian Institution, Washington, D.C. 20560-0315; jrz@nasm.si.edu.

Introduction. This report summarizes results obtained recently for mapping projects supported by NASA PG&G grant NAG5-11743. The grant identifies topical problems for both Mars and Venus, with science objectives that make use of geologic mapping results.

Mars Mapping. Geologic mapping of the Medusae Fossae Formation (MFF) on Mars was carried out in support of the science objective to identify and interpret the stratigraphic relationships within and around both eastern and western exposures of MFF near the equator of Mars, for use in evaluating specific hypotheses of origin for these unusual materials. Two Mars Transverse Mercator (MTM) quadrangles were mapped at 1:500,000 scale and combined for eventual publication at 1:1M scale on a single map sheet (white box in fig. 1). This mapping effort identified three subdivisions within both the upper (Amu) and middle (Amm) members of MFF, with clear stratigraphic contact relationships at various places within the map.

Results from the detailed mapping were recently extended to a more regional view through geologic mapping at 1:2M scale, which can be compiled at 1:4M scale (fig. 1). The three subdivisions of both the upper and middle members can be traced across much of the eastern portion of MFF. The regional mapping was aided greatly by topographic data obtained from the Mars Orbiter Laser Altimeter (MOLA) through collaborators H. Frey and S. Sakimoto. The MOLA data led directly to the identification of an exhumed channel below unit Amm_1 [1], which appears to be part of a collection of outflow features northwest of the Tharsis region [2]. Efforts are still underway to compile "truth tables" for the numerous published hypotheses of origin for MFF [see 3], based on both the observed properties of the martian materials and literature about terrestrial examples of the proposed mechanisms of origin. Assessments to date indicate that both the ignimbrite [4-6] and the eolian material [5, 7-9] hypotheses are the most viable alternatives with regard to the new data sets from Mars Global Surveyor (MGS). Only very recently has any internal layering been identified in Mars Orbiter Camera (MOC) images of MFF materials (fig. 2), which should prove useful in evaluating the merits of hypotheses of origin. Following submission of the combined MTM 05142 and 00142 maps and submission of the eastern regional map (fig. 1), work will begin on a western regional map covering MC-15SE and MC-23NE (15° N. to 15° S., 180° to 202.5° W.). We plan to submit a manuscript to JGR later this year that will summarize our efforts at evaluating the many MFF hypotheses of origin.

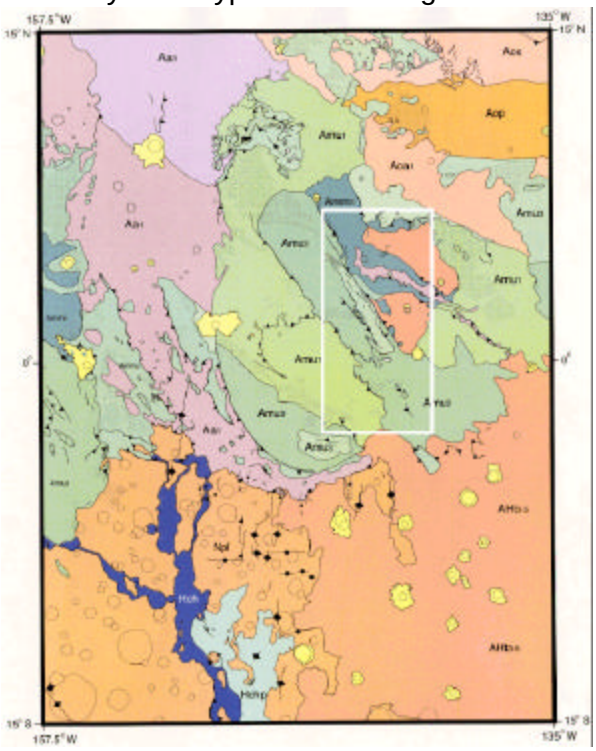

Figure 1. Regional geologic map of the eastern portion of MFF, corresponding to MC-8SE (top half) and MC-16NE (bottom half). Mapping carried out at 1:2M scale, to be published at 1:4M scale. White box shows location of MTM 05142 and 00142 (7.5° N. to

2.5° S. , 140° to 145°W.), to be published at 1:1M scale.

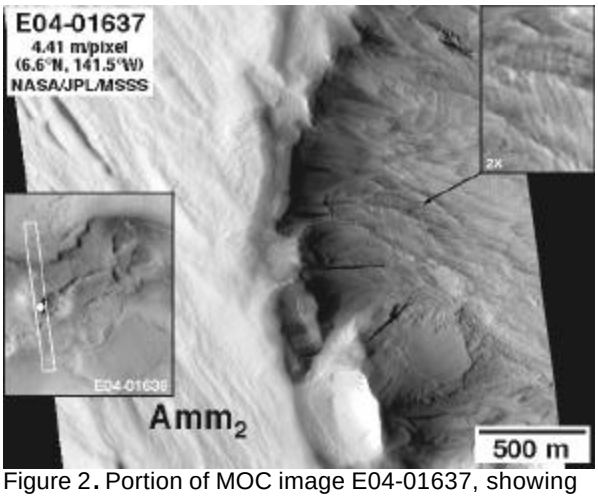

Figure 2. Portion of MOC image E04-01637, showing horizontal layering (enlarged at upper right) exposed within MFF unit Amm_2. Inset shows image context.

Venus Mapping. Venus mapping efforts are in support of the science objective of identifying and interpreting stratigraphic relationships in the northern lowland plains of Venus, to provide constraints on global resurfacing models. Geologic mapping of the Kawelu Planitia quadrangle (V-16) on Venus is now complete, compiled at a scale of 1:5M based on mapping at FMAP scale that preserves the full resolution of the Magellan SAR data. A revised version of the V-16 map should be submitted by the end of the summer; no unit boundaries changed on the map, but the correlation chart underwent considerable change following discussion at the 2001 mappers meeting. Detailed stratigraphic information was extracted from the V-16 map for lobate plains flow units around the Sekmet Mons volcano, which provides new insights into the possible resurfacing of the northern lowland plains; this work is described in a manuscript to be submitted to JGR-Planets this summer [10]. Experience gained in revising the V-16 map was crucial to carrying out the new mapping. A preliminary geologic map of the Bellona Fossae quadrangle (V-15; fig. 3, immediately west of V-16) was presented both at a special session at the Spring AGU [11] and at the 2002 mappers meeting.

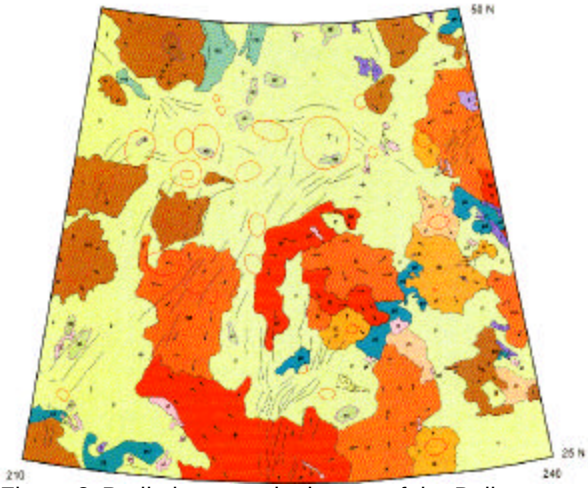

Figure 3. Preliminary geologic map of the Bellona Fossae quadrangle (V-15), Venus. Mapping was carried out at 1:5M scale. See fig. 4 for stratigraphy.

Fewer stratigraphic relationships are evident among the lobate plains in V-15 than were observed in V-16, but local volcanic centers do preserve a sequence of volcanic flow emplacements. This information is represented in the correlation chart for the V-15 map (fig. 4), which also illustrates the style of correlation chart devised for the revised V-16 map. Regional plains, lacking distinctive attributes in the Magellan SAR data or other remote sensing data sets, are abundant in both the V-15 and V-16 quadrangles. However, at present there is no way to verify (or to test) that the regional plains are the same materials within each quadrangle, let alone across the adjacent quadrangles.

The correlation chart is a compromise in an attempt to portray stratigraphic information that is consistent within a given quadrangle, but also to show readers the considerable uncertainty associated with each unit. An outcome of the 2002 mappers meeting was a decision to attempt to clarify what each mapper intends to show by their correlation charts. The GEMS working group will coordinate the compilation of the correlation chart information, in order to provide better understanding (if not uniformity) between charts of different maps.

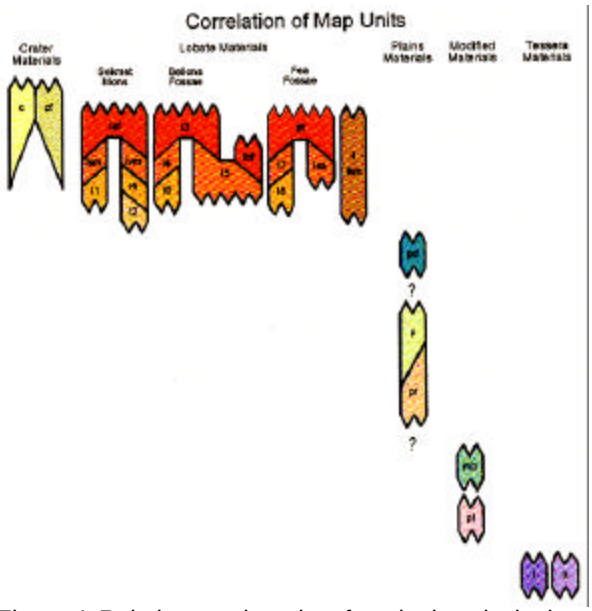

Figure 4. Relative stratigraphy of geologic units in the V-15 map (fig. 3). Hachured lines indicate uncertainty in vertical extent of unit, but relative vertical position is consistent with mapped relationships found within the V-15 map. Sloping lines indicate time-transgressive contact between units.

References. [1] J.R. Zimbelman and others, Geol. Soc. Am. Abs. Prog., 32(7), A303, 2000. [2] J.M. Dohm and others, JGR-Planets, 106(E6), 12301-12314, 2001. [3] J.R. Zimbelman and others, LPS XXX, Abs. #1652, LPI (CD-ROM), 1999. [4] Scott, D.H., and K.L. Tanaka, JGR, 87, 1179-1190, 1982. [5] Scott, D.H., and K.L. Tanaka, U.S.G.S. Misc. Invest. Series Map I-1802-A, 1986. [6] M.G. Chapman and others, U.S.G.S. Misc. Invest. Series Map I-1962, 1989. [7] Ward, A.W., JGR, 84, 8147-8166, 1979. [8] Carr, M.H., Water on Mars, pp. 133-6, Oxford Univ. Press, New York, 1996. [9] Wells, G.L., and J.R. Zimbelman, Arid Zone Geomophology, 2nd ed. (D.S.G. Thomas, Ed.), pp. 659-690, Wiley & Sons, New York, 1997. [10] Zimbelman, J.R., Flow field stratigraphy surrounding Sekmet Mons volcano, Kawelu Planitia, Venus, submitted to JGR-Planets. [11] Zimbelman, J.R., Eos, Trans. AGU, 83(19), Spring Meeting Suppl., Abs. #P21A-02, 2002.

EVOLUTION OF WESTERN HESPERIA PLANUM, MARS: GEOLOGIC MAPPING OF MTM QUADRANGLES -14257 AND –20257

T.K.P. Gregg[1] and D.A. Crown[2] [1]Dept. of Geology, 876 NSC, University at Buffalo, Buffalo, NY 14260-3050; (716) 645-6800; tgregg@nsm.buffalo.edu; [2]Planetary Science Institute, 620 N. 6th Ave., Tucson, AZ 85705; crown@psi.edu.

Objectives. Although Hesperia Planum stratigraphically defines the base of the Hesperian System, its western boundary remains poorly defined. We are conducting detailed geologic mapping to constrain the transition from western Hesperia Planum, through Tyrrhena Patera (~22° S., 252° W.), to the adjacent Noachian-aged cratered highlands. Most of this transition is included in MTM –15257 and –20257 quadrangles. Specifically, we are addressing the following questions.

1. What is the stratigraphic relation between Tyrrhena Patera shield materials and Hesperia Planum? What is the stratigraphic relation between the Noachian highlands west of Hesperia Planum and Tyrrhena Patera?

To the east of the Tyrrhena Patera summit, the ridged plains material of Hesperia Planum embays the older shield materials of Tyrrhena Patera [1,2]. However, to the west of Tyrrhena Patera, the relationship is much less clear [2]. Answering the questions posed here has significant implications for the duration and style of volcanic activity at Tyrrhena Patera, and the precise crater size-frequency distributions that have been used to define the base of the Hesperian System [3]. We plan to carry out 1:500,000 geologic mapping west of the Tyrrhena Patera summit (MTM –15257 and –20257 quadrangles) to address these issues.

2. What is the nature of the materials found west of the Tyrrhena Patera summit region (but still included within the ridged plains material of Hesperia Planum, as mapped by Greeley and Guest [4])? How and when has it been eroded and mantled?

Greeley and Crown [1] and Gregg and others [2] identified materials west of the Tyrrhena Patera summit region that appeared to be associated with the volcano, but the precise relation remains unclear. Greeley and Crown [1] called it “Hesperian-aged smooth plains material,” and suggested that it could be a facies unit of the ridged plains or an eruptive unit associated with Tyrrhena Patera that is part of, or underlies, the shield materials. Gregg and others [2] termed this same material “etched plains,” and did not suggest a specific origin, but stated that it had a “complex history” and that it is younger than the shield materials adjacent to the Tyrrhena Patera summit region. Understanding the origin and age of this material would reveal important information about the evolution of volcanism, volatiles, and climate in this region.

Significance. Tyrrhena Patera (22° S., 253° W.) is northeast of Hellas basin and on the western edge of Hesperia Planum. The erosional morphology of the patera's ancient shield suggests it is composed of friable, fine-grained materials, such as pyroclastic deposits [1,2,5]; although valley morphology suggests that there may be buried lava flows in the volcano’s flanks [6]. Investigation of the Tyrrhena Patera shield materials provides a unique opportunity to constrain the interaction of rising magma through the crust of the ancient cratered southern highlands.

Crater size-frequency distributions for Hesperia Planum define the global base of the Hesperian System. The crater statistics compiled for Hesperia Planum [3] were based on the boundaries of Hesperia Planum as defined by Greeley and Guest [4]. Greeley and Crown [1], Crown and others [7] and Gregg and others [2] demonstrated that the large lava flow field associated with Tyrrhena Patera is actually younger than Hesperia Planum, although it was included as part of Hesperia Planum by Greeley and Guest [4]. In contrast, the shield materials associated with Tyrrhena Patera are older than Hesperia Planum

[1,2]. Although the precise boundaries of Tyrrhena Patera volcanic deposits are not yet clearly defined, they cover a large area originally included as part of Hesperia Planum [4]. Crater statistics for Hesperia Planum [3]—and the base of the Hesperian System—may therefore be erroneous. It is important to clarify the boundaries of geologic units in the western Hesperia Planum region to accurately constrain the timing of events here, and, by analogy, elsewhere on Mars as well.

Tyrrhena Patera and Hesperia Planum. Tyrrhena Patera deposits were originally mapped as fully contained within Hesperia Planum [11]; recent mapping [2,4] reveals that the boundary between Hesperia Planum and Tyrrhena Patera is complex. Within the MOLA data, a continuously sloping surface is observed from the summit of Tyrrhena Patera for ~500 km to the west and north. This suggests that Tyrrhena Patera shield materials extend hundreds of kilometers farther than previously observed, covering several thousand square kilometers of what was originally believed to be ridged plains of Hesperia Planum [4]. Hesperia Planum deposits embay Tyrrhena Patera shield materials to the east, but investigations of MOLA topography suggest that portions of Hesperia Planum adjacent to Tyrrhena Patera are significantly higher than the rest of Hesperia Planum. We interpret this to be caused by local mantling of Hesperia Planum, possibly by Tyrrhena Patera shield materials. The mantling material may be juvenile volcanic products, suggesting prolonged explosive activity at Tyrrhena Patera, or reworked shield materials.

This has implications for the eruption and emplacement style of the deposits: how much of the shield materials at Tyrrhena Patera are comprised of air fall deposits, and how much was emplaced via pyroclastic flow? Wilson and Walker [8] determined that the emplacement of air fall deposits at a central vent volcano is primarily a function of the height of the eruptive plume [9]. Plume height is dependent upon such factors as vent radius, particle and gas densities, exit velocity, volatile content, mass eruption rate, and atmospheric temperature and density [8, 10-13]]. The width of a plinian eruption cloud, which is the same as the maximum distance from the vent at which deposition takes place, is approximately equal to the eruption cloud height. The dynamics of explosive eruptions and the behavior and stability of the resulting eruption plumes on Mars have been theoretically analyzed by Wilson and Head [14, 15]. Depending on magma volatile content, the maximum eruption cloud height would be 250–350 km [16]. Glaze and others [9,17] are examining how these models can be improved in an effort to better constrain eruption parameters on Mars and Io.

Alternatively, the deposits to the west of Tyrrhena Patera may be pyroclastic flows. Greeley and Crown [1] estimated the runout distance of martian pyroclastic flows around Tyrrhena Patera. They concluded that initial velocities of ~250 m/s to 650 m/s are required to create the etched plains materials via pyroclastic flow emplacement. These velocities are 4 to 5 times higher than any observed terrestrial flow [18] but correspond with velocities obtained based on theoretical considerations [10, 19]. Comparing such model results with measured deposit distributions and thicknesses (using MOLA and VO images) would allow us to determine how much of the volcano is constructed of air fall deposits versus pyroclastic flows.

The etched plains material may not be a primary pyroclastic deposit at all, but instead may be a reworked and re-deposited granular material. Because Tyrrhena Patera is the nearest large source of granular material (in the form of pyroclastics), it may be difficult to distinguish reworked pyroclastic deposits from primary deposits. We will search for continuity in topographic benches in these deposits with those observed in the Tyrrhena Patera lower shield materials: the

topographic benches in the shield materials have been interpreted to be created by distinct cooling (welding) units [20]. Lateral continuity into the etched plains material would support a pyroclastic origin and increase the area over which volcanic deposition occurred.

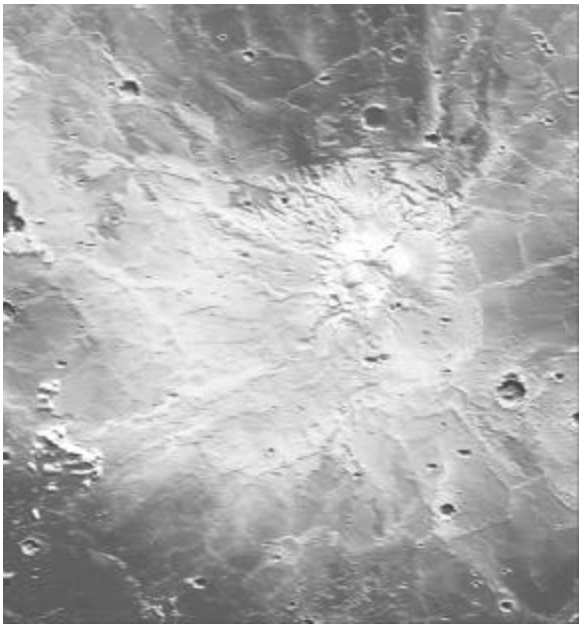

MOLA image of Tyrrhena Patera; north is at the top. The summit (white and light gray) reflects the highest topography in the region. Note the continuous slope from the summit to the relatively high terrain to the west. The relatively low-lying ridged plains represent Hesperia Planum to the east; the nature of the materials north and west of the summit remains enigmatic. Image is ~600 km wide.

Implications. The crater size-frequency distributions that define the base of the Hesperian System were generated using the boundaries of Hesperia Planum as defined by Greeley and Guest [4] on a 1:15,000,000 geologic map [Tanaka and others, 1986]. However, the boundaries of eastern Hesperia Planum have changed considerably since then as a result of work by Crown and others [1,2,20,21]. By mapping MTM –20257 and –15257 quadrangles, we will better define the boundaries of Hesperia Planum, Tyrrhena Patera, and the surrounding plains. This may ultimately lead to a reformulation of the cratering statistics used to define the base of the Hesperian System.

References. [1] Greeley R. and Crown D.A. (1990) *JGR, 95*, 7133-7149. [2] Gregg T.K.P. and others (1998) *USGS Misc. Invest. Ser. Map I-2556*. [3] Tanaka, K. (1986) PLPSC 17th, E139-158. [4] Greeley, R. and J.E. Guest (1987) *USGS Misc. Invest. Ser. Map* [5] Crown, D.A. and others (1992) *Icarus 100*:1-25. [6] Gulick V.C. and Baker V.R. (1990) *JGR, 95*, 14,325-14,344. [7] Crown and others (1991) *LPSC XXII*:261-262. [8] Wilson, L. and G.P.L. Walker (1987) *Geophys. J.R. Astron. Soc. 89*:657-679. [9] Glaze, L.S. and S.M. Baloga (2000) *J. Geophys. Res 105*:17,579-17,588. [10] Sparks, R.S.J. and L. Wilson (1976) *J. Geol. Soc. London 132*:441-451. [11] Wilson, L. and others (1978) *J. Geophys. Res. 83*:1829-1836. [12] Valentine, G.A. and K.H. Wohletz (1989) *J. Geophys. Res. 94*:1867-1887. [13] Bursik, M.I. and A.W. Woods (1991) *J. Volcanol. Geotherm. Res. 45*:347-350. [14] Wilson, L. and J.W. Head (1981) *J. Geophys. Res. 86*:2971-3001. [15] Wilson, L. and J.W. Head (1994) *Rev. Geophys.* 32:221-263. [16] Mouginis-Mark, P.J. and others (1988) *Bull. Volcanol. 50*:361-379. [17] Glaze, L.S. and S. Baloga (2001) *Lun. Planet. Sci. Conf. XXXII*:#1209. [18] Kieffer, S.W. (1981) *U.S. Geol. Surv. Prof. Pap. 1250*:379-400. [19] Sparks, R.S.J. and others (1978) *J. Geophys. Res. 83*:1727-1739. [20] Crown D.A. and R. Greeley (1993) *JGR, 98*, 3431-3451. [21] Mest, S.C., and D.A. Crown **(**2002) *U.S. Geological Survey Geologic Investigations Series Map I-2730*, in press.

MGS-BASED TOPOGRAPHIC ANALYSIS OF THE SOUTH POLAR LAYERED DEPOSITS OF PLANUM AUSTRALE, MARS

E.J. Kolb[1] and K.L. Tanaka[2], [1]Dept. of Geological Sciences, Arizona State University, Tempe, AZ 85287-1404, eric.kolb@asu.edu, [2]Astrogeology Team, U.S. Geological Survey, 2255 N. Gemini Dr., Flagstaff, AZ 86001, ktanaka@usgs.gov

Introduction. South pole Amazonian geology is dominated by the formation and modification of the south polar layered deposits (SPLD) of Planum Australe. Mars Global Surveyor-based regional geologic mapping of the planum at 1:3,000,000 scale, coupled with geomorphic and topographic analyses of localized features are enhancing our understanding of the formation and modification history of the SPLD. Previous regional geologic maps of the south pole were compiled from Mariner 9 images at 1:5,000,000 scale by [1] and from medium-resolution Viking images at 1:15,000,000 scale by [2].

Results. The deposits of Planum Australe are offset from the pole by ~2° and are asymmetrically distributed between latitudes 70° and 80° S. [2, 3]. The SPLD lie upon highland terrain, including part of the rim of Prometheus basin, at an elevation ~6 km higher than the northern cap. The crest of Planum Australe occurs within the residual ice deposits (87° S., ~10° E.), where a broad dome is present with over 3 km of relief at one end of the cap [3]. Dissecting both the permanent CO_2 ice cap and underlying SPLD are the extensive spiral troughs observed from the edge of the cap at 0° W. outward to ~ 82.5° S.

The SPLD topography at <82.5° S., 125-230° W. is markedly different from that closer to the pole. Here, broad plateaus, semi-arcuate east-west-trending ridges, and partly buried craters characterize the regional topography. The exposed rims of partly buried craters associated with underlying highland materials is seen at several locations within the interior of the Ultimi lobe, including the ~72-km-diameter "snowman crater" at 75° S., 212° W. Between 110° and 120° W., <300-meter-thick sequences of SPLD extend poleward up to 150 km from the distal margins of Planum Australe. Within this region, numerous partly buried craters and semi-arcuate ridges are observed. Sections of the arcuate ridges often overlie and extend tangentially from partly buried crater rims, whereas others do not appear associated with buried craters. The extending ridges commonly link up with other such ridges to form lengthy cuspate ridge systems. Several of the ridges extend across the very distal edges of Planum Australe (for example, 77° S., 140° W.). Generally, the northern sides of the ridges are bounded by troughs, which commonly expose underlying highland material where the SPLD are thin. Slope values derived from MOLA Digital Elevation Maps indicate that the equator-facing sides of the ridges are steepest, commonly sloping between 6.5° and 20°. Other small to large ridges and bumps of various orientations also locally mark this area of the SPLD. MOC narrow- and wide-angle images of the ridges indicate that they are composed of layered sequences of SPLD. Although [4] has attributed these semi-arcuate ridges to potential bi-modal wind regimes, the ridges may instead be unusual erosional remnants of a once thicker PLD in this area.

References. [1] Condit, C.D., and Soderblom, L.A. (1978) USGS Map I-1076. [2] Tanaka K.L. and Scott D.H. (1986) USGS Map I-1802C. [3] Smith, D.E. and others (1999) Science 284, 1495-1503. [4] Howard, A.D. (2000) Icarus 144, 267-288.

GEOLOGIC MAPPING OF THE METIS REGIO QUADRANGLE (V-6), VENUS

James M. Dohm[1] and Kenneth L. Tanaka[2]; [1]Department of Hydrology and Water Resources, University of Arizona, Tucson, AZ, 85721; [2]U.S. Geological Survey, Flagstaff, AZ 86001

Introduction. The Metis Regio quadrangle (V-6) in the northern hemisphere of Venus (50° to 75° N., 240° to 300° E.) includes a variety of coronae, large volcanoes, ridge belts, and other volcanic and structural features distributed among regional plains materials, affording study of their detailed age relationships and evolutionary development. Coronae in particular have tectonic, volcanic, and topographic signatures that indicate complex evolutionary histories. The main purpose of this geologic map is to reconstruct the volcanic and tectonic histories of the Metis Regio quadrangle at 1:5,000,000 scale. We document five partly overlapping stages of geologic activity that resulted in (from oldest to youngest): (1) tessera materials, (2) corona materials that form concurrently with older volcanic plains-forming materials but are embayed in most places by younger volcanic plains materials, (3) isolated corona materials that were formed along structure belts and subsequently covered by volcanic flows which were in turn reactivated and deformed locally as a result of late-stage relaxation of the features or reactivation of basement structures resulting from a nearby episodically active coronae, and (4 and 5) four large volcanic constructs (Mnemosyne Regio, Metis Regio, Mokosha Mons, and Atira Mons), shield and lava flow fields, patches of smooth plains material, and impact crater materials.

The geologic map information of the Metis Regio region was initially compiled on photographic prints of ten full-resolution (75 m/pixel) Magellan SAR mosaics at 1:1,500,000-scale produced by the U.S. Geological Survey. This mapping was then scanned, reprojected, vectorized, and merged into a Geographic Information System format that was edited to register it to the 1:5,000,000-scale quadrangle base. The transferal of F-MAP resolution data to the quadrangle base resulted in greater accuracy of the placement of contacts.

Stratigraphy. We distinguish 34 geologic units in the Metis Regio quadrangle based on stratigraphic relations, morphologic characteristics, and radar properties. These units consist of materials of various ages and geologic associations forming tesserae, coronae, widespread older and younger plains modified by varying degrees and styles of tectonic structures, volcanoes, domes, lava flows, and impact craters. Our geologic mapping indicates five stages of major geologic activity for the Metis Regio quadrangle of Venus. Except for tessera, the map units and structures are not all unique to a particular stage of major geologic activity. Rather, the stages represent peak periods in the type of geologic activities that produced the dominant materials and features for each stage. Generally, the geologic sequence in this quadrangle agrees with previous studies of regional and global stratigraphies that apply to this region [1-5]. The following discussion expounds on the geologic activity for each of the five major stages.

Stage 1. The oldest materials in the V-6 quadrangle consist of isolated patches of tessera material that crop out through various plains materials; in places, tessera material is transitional with older corona and plains materials deformed by similar complex structure. Tessera material records the earliest and largest degree of structural deformation in the map region; various models have been proposed to account for the recorded crustal deformation. The complex structural history of tessera material in the Metis Regio region is difficult to unravel and may include regional and global strain, including deformation from numerous centers of magmatic activity.

Stage 2. During this stage, coronae formed contemporaneously with patches of plains units 1 and 2 as a result of magma plumes and convection cells blistering the

surface of the map region. Corona development included dense radial and concentric fracturing and faulting, dike emplacement, ridge development, and volcanism resulting in densely lineated and ridged terrain (in some cases, very similar to some of the tessera outcrops). The structures marking most outcrops of this stage are more than an order of magnitude denser than the structures that deform younger plains materials. In some cases, structure belts made up of undifferentiated plains materials may have formed concurrently with the coronae. Structure belts may also mark reactivated preexisting zones of lithospheric weakness, perhaps related to a phase of tectonism prior to a proposed global volcanic resurfacing event. Coronae and structure belts may have been active for most of the recorded geologic history of the Metis Regio region, though activity waned and became more localized after Stage 2.

Stage 3. Widespread plains materials partly buried and/or embayed Stage 1 and 2 materials, including inactive, older parts of coronae and structure belts. During this stage, extensional and contractional tectonism diminished, including structure belt development, except for local reactivation that may have resulted from global to local stresses, including relaxation of the crustal/lithospheric materials and/or resurgence of activity at one of the nearby magmatic-driven centers of activity (for example, coronae). In addition, plains-forming materials were deformed by contractional tectonism, which resulted in wrinkle ridges.

Stage 4. Emplacement of voluminous fissure-fed eruptions and major central volcanism resulted in more extensive plains-forming materials and in large shield volcanoes, Atira Mons, Mokosha Mons, Metis Regio, and Mnemosyne Regio, respectively. The detailed geologic mapping indicates more than one episode of volcanism for some of the large shields. Other investigators have noted that broad shield volcanoes are stratigraphically some of the youngest features on Venus [6-8].

Stage 5. Continued emplacement of smooth plains materials and shield field materials, continued growth of the large shield volcanoes, possible activity at some of the coronae, other local volcanism and tectonism, wind-driven activity, and impact cratering account for the youngest activity of the map region.

Overall, the transition from earlier, much more intensive magmatic-driven tectonic activity to widespread plains volcanism and waning tectonism and finally to large volcanic constructs, domes, and extensive lobate flow fields documented in the Metis Regio quadrangle of Venus is similar to the volcanotectonic evolution proposed globally for Venus [2-4] as well as documented for the Tharsis region of Mars [9-11]. The volcanotectonic evolution for both planets has been proposed to be the result of stagnant-lid convection, persisting for more than 3 billion years for Mars and less than 500 million years for Venus [12-14].

References. [1] Stofan E.R. and Head J.W., 1990, Icarus 83, 216-243. [2] Tanaka K.L. and others, 1997, in Venus II (UA Press, Bougher and others, eds.), p. 667-694. [3] Basilevsky A.T. and others, 1997, in Venus II (UA Press, Bougher and others, eds.), p. 1047-1084. [4] Basilevsky A.T. and Head J.W., 2000, Planet. Space Sci. 48, 75-111. [5] Ivanov M.A. and Head J.W., 2001, J. Geophys. Res. 106, 17,515-17,566. [6] Namiki N. and Solomon S.C., 1994, Science 265, 929-933. [7] Price M. and Suppe J., 1994, Nature 372, 756-759. [8] Basilevsky A.T. and Head J.W., 2000, J. Geophys. Res. 105, 24,583-24,611. [9] Scott D.H. and Tanaka K.L., 1986, USGS Map I-1802-A. [10] Anderson R.C. and others, 2001, J. Geophys. Res., 106, 20,563-20,585. [11] Dohm J.M. and others, 2001, J. Geophys. Res. 106, 32,943-32,958. [12] Strom R.G. and others, 1994, J. Geophys. Res. 99, 10,899-10,926. [13] Solomatov V.V. and Moresi L.N., 1996, J. Geophys. Res. 101, 4737-4753. [14] Sleep N.H., 2000, J. Geophys. Res. 105, 17,563-17,578.

LAKSHMI PLANUM QUADRANGLE (V-7) VENUS: RESULTS OF PRELIMINARY MAPPING

M.A. Ivanov[1,2] and J.W. Head[2]. [1]Vernadsky Institute, RAS, Moscow, Russia, mishaivn@mtu-net.ru, [2]Dept. of Geological Sciences, Brown University, Providence, RI, USA, james_head_iii@brown.edu.

Introduction. Lakshmi Planum dominates the western portion of Ishtar Terra and represents one of the most spectacular features on Venus [1]. Lakshmi Planum is a high-standing (about 3-4 km above MPR) plateau surrounded by the highest venusian mountain ranges. The surface of the plateau is covered by morphologically smooth plains and two significant volcanic centers; Colette and Sacajawea Paterae occur in the middle of the plains. The unusual characteristics of Lakshmi Planum have led to a variety of interpretations of its mode of origin ranging from the hot spot to collision hypotheses [2,3 and reference therein]. The V-7 quadrangle portrays the planum itself and its surroundings (fig. 1). The mapping in this area allows us to document specific features of Lakshmi Planum and establish the sequence of events in the formation and evolution of this major feature on Venus. As the first stage of our mapping project we undertook reconnaissance mapping within the V-7 quadrangle in order to outline the principal features in this area and develop a preliminary model of the sequence of events there.

Topographic and stratigraphic characteristics of major features within the V-7 quadrangle. Lakshmi Planum, which is about 2,000 km across, occupies the northern half of the V-7 quadrangle. A broad zone of complexly deformed terrain surrounds the roughly circular structure of Lakshmi Planum at the intermediate elevation (fig. 1). In the south, two major scarps, Vesta Rupes in the north and Ut Rupes to the south, define this zone. The major features of this transition zone are small fragments of tessera terrain (for example, Clotho Tessera) and linear belts of grooves. The lava plains of the lowland of Sedna Planitia, the surface of which is topographically flat, broadly embay these terrains. The southeastern corner of the quadrangle is occupied by numerous lava flows of Neago Fluctus. The flows emanate from Muta Mons at intermediate elevation and flow down toward the vast lowland of Sedna Planitia. The flows embay the terrains of the transition zone and the surface of Sedna Planitia as well. In the west, large Omosi-Mama Corona, which is the source of the apparently young Djata Fluctus, is the main feature of the transition zone. Large tessera massifs, Atropos Tessera and Itzpapalotl Tessera (out of the V-7 area), make a giant arc that embraces Lakshmi Planum from the northwest, north, and northeast.

The most important features of Lakshmi Planum are mountain belts that make an almost complete zone outlining the relatively flat interior of the plateau (fig. 1). The range of Danu Montes borders the southern edge of the plateau. Danu Montes form a wide arc (about 1,500 km long) the top of which is about 1.5-2 km above the surface of Lakshmi Planum. The highest point of the montes is around 335° E. and the height of the range is lower toward the eastern and western edges. The southwestern sector of Lakshmi Planum between about 60-65° N. shows little evidence for mountain belts, but the western and northwestern edges of the planum are bordered by the mountain range of Akna Montes. Akna Montes make a compact zone (about 1,000 km long and 250 km wide) with the highest area between 65-70° N. that stands about 3 km above the surface of Lakshmi Planum. The northern and partly northeastern edges of the planum are bordered by Freyja Montes, which stand about 3-3.5 km higher than the adjacent surface of Lakshmi. The range of Freyja Montes consists of latitudinal and longitudinal branches. The first is short, wide (about 500 km long and 200-300 km wide), higher, and straight. The second is smaller in all respects and is slightly convex to Lakshmi Planum. These mountain

ranges, as well as Maxwell Montes (outside of V-7), consist of tightly packed elongated parallel ridges 5 to 10 km wide and resemble to some extent the common ridge belts elsewhere on Venus [4]. At the contacts with the interior plains of Lakshmi Planum, there is abundant evidence for embayment of the mountain by the plains. At the longitudinal branch of Freyja Montes, however, the interior plains appear to be slightly ridged, conformal to the strike of the mountain belt.

The interior surface of Lakshmi Planum is generally flat, slightly tilted toward the south and lacks significant tectonic structures such as those that are very abundant at the edges and outside of the planum. The interior of Lakshmi displays three types of materials. The most widespread are plains with moderate and uniform radar albedo and deformed by a network of wrinkle ridges. Morphologically, these plains represent a complete analog to regional plains of Venus [5,6] that occur, in particular, on the surface of Sedna Planitia. Stratigraphically lower than the intra-Lakshmi regional plains are materials heavily deformed by tectonic structures. Although these materials are not in direct contact with the mountain ranges, within both Akna and Freyja Montes there are inclusions of similar materials embedded by the ridges of the mountain belts. Stratigraphically higher than the regional plains within Lakshmi are volcanic plains consisting of numerous radar brighter and darker flows that bear almost no tectonic deformation. The flows are clearly related to two major volcanic centers, Colette and Sacajawea Paterae, and are analogous to the youngest lava plains on Venus that surround distinct centers such as large volcanoes [7-10].

Sequence of events. Our first-order observations and preliminary mapping within the V-7 quadrangle are summarized as the following general and tentative sequence of events during the formation and evolution of Lakshmi Planum: (1) The oldest features within the area of our mapping appear to be the heavily tectonized materials that are embayed by the intra-Lakshmi regional plains. (2) The mountain belts and the transition zone of complexly deformed terrains around Lakshmi may be somewhat younger but very detailed mapping is necessary to establish an order of events among these features. (3) The mountains and the transition zone are embayed by vast regional plains both from inside (within Lakshmi Planum) and outside (in Sedna Planitia). Neither in Lakshmi Planum nor outside is there evidence for the sources of these plains. (4) The latest activity within the area under study was volcanism at several distinct centers that produced the lava flows of Neago Fluctus and Djata Fluctus to the southeast and west of Lakshmi and around Colette and Sacajawea Paterae within the planum.

References. [1] Barsukov, V.L., et al., JGR, 91, D399-D411, 1986, [2] Kaula, W.M., et al., JGR, 97, 16085-16120, 1992, [3] Kaula, W.M., et al., Ishtar Terra in: Venus II Geology, Geophysics, Atmosphere, and Solar wind environment, S.W.Bougher, D.M. Hunten, and R.J. Phillips eds., Univ. Arizona Press Tucson, 789-900, 1997, [4] Banerdt W.B., et al., Plains tectonics on Venus in: Venus II Geology, Geophysics, Atmosphere, and Solar wind environment, S.W.Bougher, D.M. Hunten, and R.J. Phillips eds., Univ. Arizona Press Tucson, 901-930, 1997, [5] Head, J.W. and A.T. Basilevsky, Geology, 26, 35-38, 1998, [6] Basilevsky, A.T. and J.W. Head, JGR, 103, 8531-8544, 1998, [7] Price, M., , et al., JGR, 101, 4657-4671, 1996, [8] Namiki, N. and S.C. Solomon, Science, 265, 929-933, 1994, [9] Ivanov, M. A. and J. W. Head, JGR, 106, 17515-17566, 2001, [10] Ivanov, M. A. and J. W. Head, Geologic map of the Lavinia Planitia (V55) quadrangle USGS Geol. Inv. Ser., Map I-2684 2001.

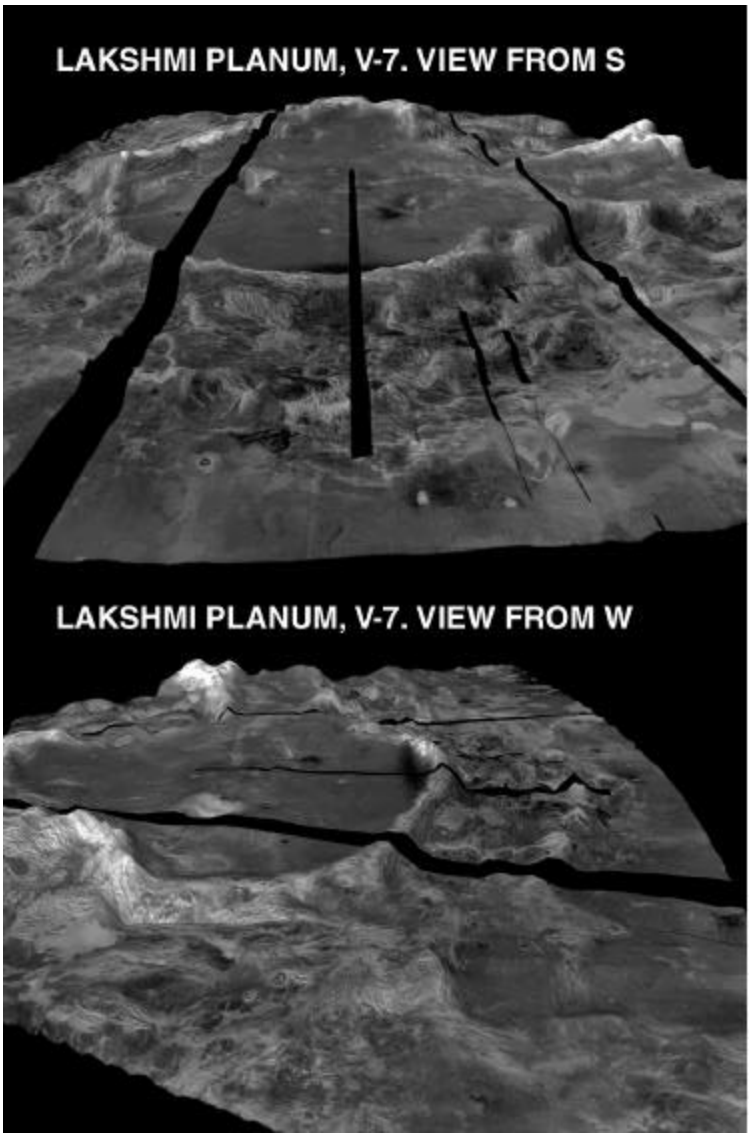

Figure 1. Two perspective views of Lakshmi Planum and its surroundings within the V-7 area. Vertical exaggeration is about 1:50.

GEOLOGIC MAPPING OF THE MEAD QUADRANGLE (V-21), VENUS

Bruce A. Campbell and David A. Clark, Center for Earth and Planetary Studies, Smithsonian Institution, Washington, DC, 20560-0315 (campbellb@nasm.si.edu).

Overview. The Mead quadrangle is bounded by lat 0°-25° N., long 30°-60° E. Mead is a 280-km-diameter impact crater (the largest on Venus), at 12.5° N., 57.4° E. Eastern Eistla Regio, which dominates the central portion of the quadrangle, contains at least seven areas of intense tectonic deformation typical of corona rim materials. Isolated, heavily deformed patches may be remnants of additional earlier coronae. The corona cluster is marked by extensive volcanic flooding of the surrounding plains, limited in spatial extent by the topographic highs associated with tessera blocks and dorsae to the east, west, and south, and with Bell Regio to the north. Earlier work in this region has primarily focused on the nature of the deposits surrounding Mead [1, 2] and the population of coronae as they relate to a global survey of such features [3].

Coronae. Eastern Eistla Regio is remarkable in the similarity of corona tectonic structure and the morphology of associated volcanic deposits across an area of approximately 1500x2000 km. To varying degrees, each corona is marked by an elliptical ring of tectonically deformed terrain and an elevated, stellate central region. Only at Didilia and Pavlova Coronae (fig. 1) are these features relatively complete; at other coronae we observe partial to complete burial of the outer rim materials. For some possible early coronae, only the central stellate region remains. Calakomana Corona, whose raised topography limits the southern extent of flow fields from the other coronae, is unique in having relatively little associated volcanism.

Lava flows from the coronae in Eastern Eistla Regio have generally low to moderate radar backscatter, with morphologies ranging from sheetlike to lobate. In general, radar-bright lobate materials appear to overlie radar-dark sheetlike materials, suggesting an increase in magma viscosity (due to changes in eruption rate, temperature, or silica content) over time. This is similar to the progression observed for Nyx Mons and Nefertiti Corona in Bell Regio. Only in a few locales do we note a clear stratigraphic relationship between flows from different coronae, and these instances are insufficient to define relative ages within the cluster.

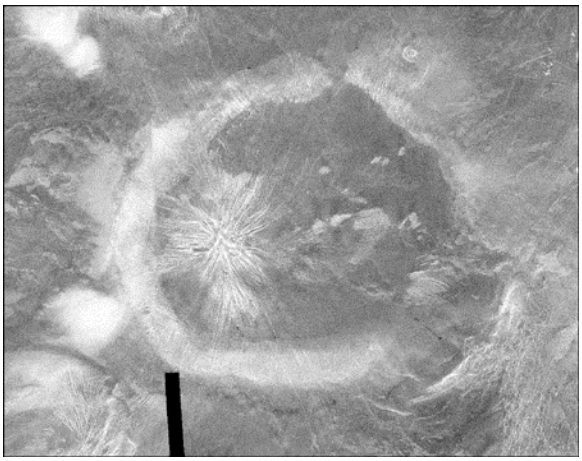

Figure 1. Pavlova Corona.

Radar-bright feathery deposits are associated with the annular rims of Didilia, Pavlova, and a remnant corona southwest of Pavlova. These very rough materials are interpreted to have formed as ground-hugging pyroclastic surges [4]. Similar deposits were mapped in central Eistla Regio [5]. The rough material overlies the corona rim fractures, though radar-dark wind streaks have mantled the surface in several areas (fig. 2). No source vents are evident, and it is not clear why such apparently volatile-rich eruptions occur along corona rims.

Central volcanoes. The largest central volcano in the map region is Dzalarhohs Mons. Smaller central edifices occur near the south, east, and northwest margins of the quadrangle. The southernmost flows from Nyx Mons extend into Akhtamar Planitia, but there is no contact between these flows and those of the corona cluster.

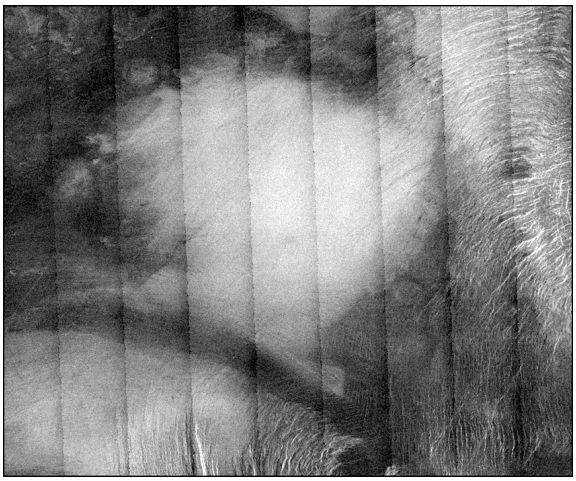

Figure 2. Radar-bright mantling deposit near margin of Pavlova Corona. Image width ~180 km. Note the radar-dark wind streaks within the bright deposit.

Impact craters. At least thirteen impact craters occur within V-21, though only Mead is greater than ~20 km in diameter. The material surrounding Mead (fig. 3) has been attributed to a variety of mechanisms, including post-impact explosive volcanism [1] and plains embayment [2]. The topography of Mead is characterized by a gentle rise from the plains up to the margins of the crater ejecta, then a downward slope across the terrace region to the crater floor. Embaying material from the plains would have to flow uphill to reach the ejecta blanket, and at that point would tend to flood portions of the crater floor. We find no evidence for explosive volcanism, and in a few locales the homogeneous materials surrounding Mead clearly behave as lavalike flows.

This work strongly suggests that the surrounding material is impact melt from the cratering event, which covers much of the near-rim ejecta. The lack of drain-back features, and the significant differences in backscatter and emissivity between the crater floor and the surroundings, further suggest that the floor materials were emplaced by post-impact volcanism. The area covered by the homogeneous materials (terraces and surrounds) is about nine times the area of the central floor (taken as the size of the transient cavity), and the total excavated depth of the crater is at least 1 km. If the average depth of the surrounding materials is 10 m, this suggests that <9% of the excavated volume was ejected beyond the cavity as melt.

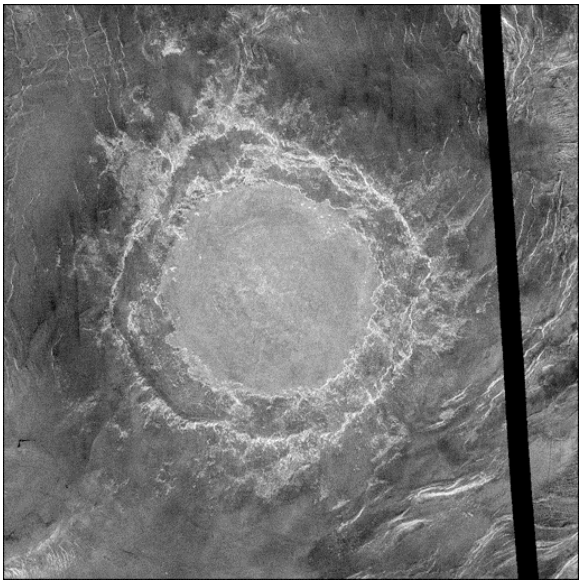

Figure 3. Mead crater (280 km diameter).

Structure. Structural deformation is dominated by wrinkle ridges that parallel major dorsae and occur concentric to the large coronae. Grabens and radar-bright fractures are often radial to corona center regions. In several cases, these radial features help to define the existence of relict coronae now largely buried by volcanic material. Wrinkle ridges are typically buried by the sheetlike and lobate flow materials of coronae, where later fractures and grabens deform these materials.

Summary. In contrast to Bell Regio to the north, eastern Eistla Regio is characterized by a nearly uniform style of volcanic activity. The dominant post-plains units are sheetlike and lobate effusive deposits, which show little morphologic difference among the various coronae. At Bell Regio, early volcanism centered on the coronalike Nyx Mons, and progressed to the more steep-sided edifices of Tepev Mons and Otafuku Tholi. Based on analysis of

flow morphology and tectonic patterns, this implied a thickening of the lithosphere and an increase in magma viscosity with time [6].

Volcanism in eastern Eistla Regio exhibits no clear progression in style with location or time. Possible (and equally plausible) interpretations are: (1) the coronae in this cluster are relatively contemporaneous, linked to a regional upwelling of material; (2) the coronae are of different ages, and reflect similar surface manifestations of independent small plumes. In either case, volcanism either stopped prior to development of steeper constructs or has not yet evolved to this stage.

References. [1] Schaber and others, JGR, 97, 13,257-13,302, 1992. [2] Herrick and Sharpton, Geology, 24, 11-16, 1996. [3] Stofan and others, JGR 97, 13,347-13,378, 1992. [4] Campbell and others, LPSC XXIX, 1998. [5] McGill, USGS Map of quadrangle V-20, in press. [6] Campbell and Rogers, JGR, 99, 21,153-21,171, 1994.

ONGOING MAPPING IN THE HESTIA RUPES QUADRANGLE (V-22) AND PRELIMINARY MAPPING OF THE IX CHEL CHASMA QUADRANGLE (V-34), VENUS

M. S. Gilmore, Wesleyan University mgilmore@wesleyan.edu and R. S. Saunders, Jet Propulsion Laboratory Ronald.S.Saunders@jpl.nasa.gov.

Introduction. We continue mapping of the Hestia Rupes quadrangle (V-22; 0°-25° N., 60°-90° E.) and have performed reconnaissance mapping of the Ix Chel Chasma quadrangle (V-34) immediately to its south (0°-25° S., 60°-90° E.). These quadrangles are centered on a portion of Ovda Regio and the adjoining plains units. A major objective of this study is to investigate plains-tessera boundaries in an effort to better understand arguably this most severe transition in volcanic and tectonic style recorded on the venusian surface. At the northern boundary of Ovda (V-22), plains embay tessera structures and are subsequently uplifted and tilted toward the plateau. This is also seen at Ovda's southern boundary (V-34), but the story here is complicated by tectonism associated with Ix Chel Chasma, which parallels and obscures the boundary. A secondary goal of the mapping is to investigate the stratigraphic position of intratessera coronae and volcanic plains.

Plains Materials of V-22. Five plains units have been defined in V-22. There are two regional plains units (fig. 1): ridged plains (unit pr) having low radar backscatter and wrinkle ridges, and deformed plains (unit pd) containing mottled flows, wrinkle ridges and fractures contributing to a higher radar backscatter (average σ_0 values are being computed).

Materials of deformed shield plains (unit pds) comprise numerous small shields, domes, and fractures; unit pds is confined to a single area and may represent the early products of the adjoining volcano Uti Hiata. Materials of ridge belt plains (unit prb) are deformed by anastomosing ridges and occur through the quadrangle. Unit prb embays tessera terrain and predates both regional plains units.

Coronae and Volcanoes. V-22 contains five named coronae and one volcano. Two coronae intersect, embay, and postdate tessera terrain. Fractures associated with H'uraru and Kaltash Coronae deform materials that are older than the regional plains unit, and materials from Ereshkigal Corona predate materials of unit pd. Habonde Corona is deformed by fractures of Kaltash and thus likely also predates regional plains.

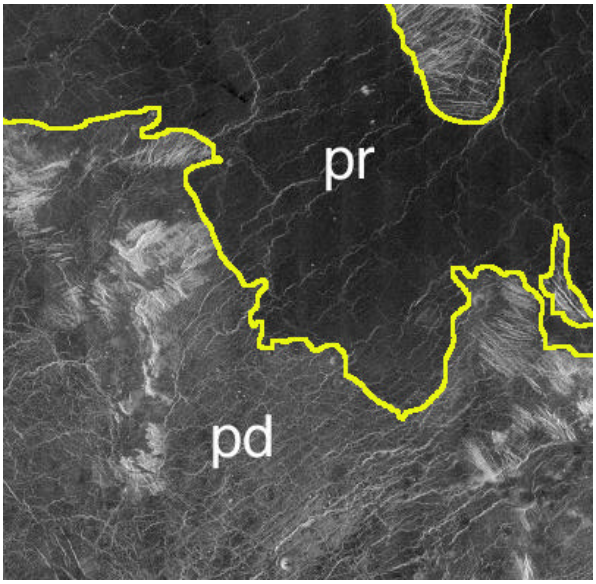

Figure 1. Regional plains units of V-22: deformed plains (pd) are embayed by ridged plains (ps).

Kunhild Corona appears to actually be a volcano; its flows and the flows of Uti Hiata Mons are the youngest in the region. We are still trying to decipher the stratigraphic position of the shield fields scattered throughout the quadrangle.

Unusual plains structures. The interpretation of plains units is made difficult in the western portion of the quadrangle by the extensive dark halo deposits of the crater Adivar and deposits of the crater Mead (west of the quadrangle) that subdue

variations in radar backscatter. Ridge belts appear to dominate this portion of the quadrangle. In two instances, the ridges converge at a topographic depression, in one case appearing to be a ridge triple junction (fig. 2). Such features may be records of localized plains subsidence early in the history of the map area.

Northern boundary of Ovda Regio. The northern boundary of Ovda Regio (78°-90° E.) is bounded by the Nayunuwi Montes fold belt, which looks very much like the folded Valley and Ridge Province of central Pennsylvania. The individual ridges within the fold belt are separated by smooth plains materials we interpret to be volcanic. Ridges of similar size and orientation are found in unit prb embaying and tilted up toward the tessera. Are plains sequentially deformed, uplifted and converted into tessera terrain at this boundary, or is this post-tessera modification as seen at Alpha Regio [1]? Detailed mapping will attempt to address this hypothesis.

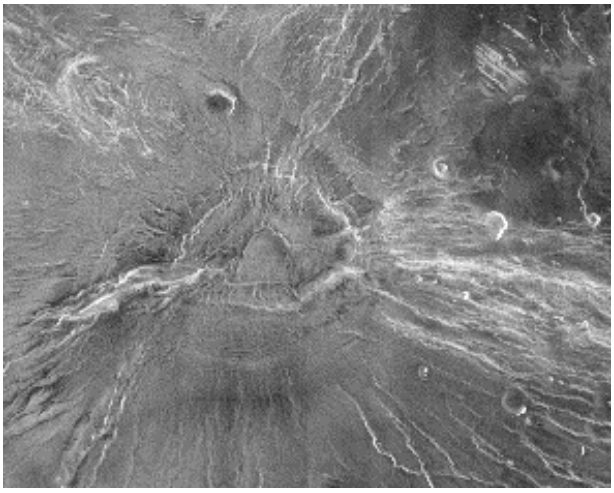

Figure 2. Convergence of ridge belts within plains. Central circular feature ~60 km across.

General stratigraphic history of V-22. The formation of the high-standing materials of tessera terrain is the first event, and some intratessera plains are cut by late-stage tessera grabens that do not extend into regional plains. Tessera terrain was embayed by plains units that have varying magnitudes and style of deformation: ridge belt plains occur throughout the quadrangle, whereas older fractured plains tend to be localized around coronae. Following embayment of the tessera and prior to the most recent volcanism, the plains were tilted up toward the margin by relative displacement upward of tessera or downward of plains [2]. At least three, and likely four, coronae were active prior to the eruption of two regional plains units. The first regional plains unit is more deformed than the second and both contain wrinkle ridges. Subsequent to plains formation, volcanic activity persisted at and was largely confined to two large edifices. The general history of the quadrangle is one of waning deformation of tessera and plains units, early corona formation, and later localization of activity at large volcanoes.

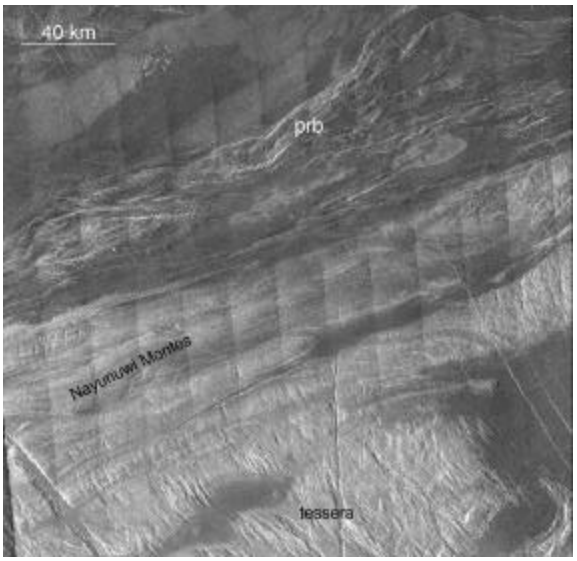

Figure 3. Plains-tessera boundary at N. Ovda. Ridges comprising edge of Ovda are of similar size and orientation as those in the ridge belt plains (prb).

Overview of V-34. As mapping for this quadrangle is in its early stages, map units are in the process of being defined and only general observations will be presented here. Tessera terrain, defined by intersecting sets of ridges and grooves and typically high backscatter, occurs in several places throughout this region. The bulk of tessera terrain in contained within Aphrodite Terra, where it contains many intratessera plains,

a concentration of which are associated with Verdandi Corona. The southwestern boundary of Manatum Tessera is embayed by regional plains, some of which have a dense coverage of structures. Several other large tessera outcrops exist in the plains in the southern portion of the quadrangle, several of which seem to grade into dorsae; that is, the tessera are adjoined by a plains unit with ridges that trend in the same direction as the intratessera ridges. All tesserae are stratigraphically oldest. The east-west-trending Ix Chel Chasma consists of a fracture belt that is superimposed on the plains-tessera boundary and severely deforms plains adjoining tessera terrain. These fractures are the source of at least four sinuous rille systems that flow downslope to the south. Two of these rilles contribute to the younger of the two recognized regional plains units. The stratigraphic position of the two coronae (Nishtigri and Aramaiti) on the southern boundary of the quadrangle is as yet unclear.

References. [1] Gilmore and Head, Met. Plan. Sci. v. 35, 667-687, 2000. [2] Saunders, R. S., LPSC 27. 1131,1996.

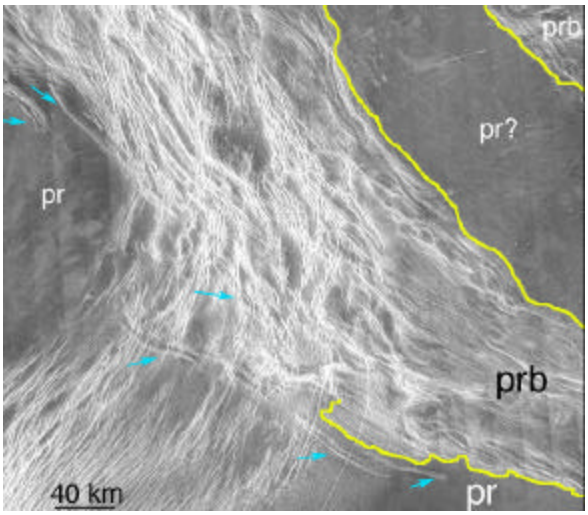

Addendum. A mapping challenge in central V-22. Materials of ridge belt plains are embayed by lavas of unit pr. Both(?) plains units are fractured in two extensional events of stress magnitude and orientation.

PRELIMINARY GEOLOGIC MAPPING OF NIOBE PLANITIA QUADRANGLE (V-23), VENUS

V. L. Hansen, Department of Geological Sciences, Southern Methodist University, Dallas, TX 75275-0395 (vhansen@mail.smu.edu); note, as of August 2002: Department of Geological Sciences, University of Minnesota Duluth, Duluth, MN 55218

Introduction. Resurfacing mechanisms are critical to the understanding of the evolution of the venusian surface [1], implications of impact crater distribution and density [2, 3], possible climatic fluctuations [4], possible effects of climate on tectonic structures [5, 6], and evolution scenarios of lithosphere-atmosphere interactions and dynamics [7]. Geologic mapping of V-23, in combination with four other contiguous VMAPS (V-37 [8], V-24, V-25 [9], and V-35 [10]) that cross the planitia of northern Aphrodite, contributes to our understanding of plains processes. In this abstract we discuss relations across V-23. Our mapping does not accept *a priori* differentiation of "plains" material; but rather, focuses on the overall history of planitia regions with attention to spatial and temporal evolution of flows and flow sources, primary and secondary structures, topography, and tectonism. To date two modes of volcanic resurfacing have emerged: relatively long and extensive flows sourced dominantly from coronae, and regional formation of a thin, lacey layer composed of coalesced small volcanic shields.

Map area. V-23 extends from 0º-25º N. and 90º-120º E., and it encompasses portions of Sogolon Planitia and Niobe Planitia, which are bounded to the south—from west to east—by crustal plateaus Ovda Regio and Thetis Regio. Ribbon-bearing tessera terrain dominates the entire southern third of the map area and extends as inliers along the eastern boundary, and also preserved as small isolated fragments across all but the northwestern-most part of the map area. Ribbon trends display regionally coherent patterns despite distances as great as 500 km locally between inliers. The large tessera tracts that comprise Ovda to the west and Thetis to the east show different but internally consistent ribbon-fold patterns with folds generally parallel to the local tessera terrain boundaries (trending NW in Ovda and NE in Thetis).

The planitia host a series of north-trending elongate basins and rises with wavelengths of 1000-1500 km. Gravity highs generally correlate with elevated topography, which preserves variably sized ridge belts, tracts of ribbon-bearing tessera terrain [11], and pervasively fractured terrain. Ridge belts trend both NE and NW in V-25 and E V-24; numerous small to large ribbon-bearing tessera terrain occur across V-23/V-24. Secondary structures including fractures and wrinkle ridges describe broad patterns across the map area.

Wrinkle ridges and fractures (locally reactivated as inversion ridges [12]) also describe regionally coherent patterns across V-23. Wrinkle ridges generally trend E to ENE, whereas fractures strike N to NNW, with local fractures striking NNE. Inversion ridges formed by filled and reactivated fractures trend parallel to the strike of adjacent fractures. In general, neither the wrinkle ridges nor the regionally coherent fractures parallel the trend of tessera ribbon structures, although locally ribbons appear reactivated along ribbon-parallel fractures.

V-23 hosts five small coronae (diameters range from 100-225 km). Each of the coronae has topographically low interiors as illustrated clearly in synthetic stereo data. Small shields generally formed later during corona formation cluster in the interior of each corona.

V-23 hosts tens to hundreds of thousands of shields. Shields are small (1-15 km diameter) quasi-circular to circular radar-dark or -bright features with or without topographic expression (shield, dome, cone, flat-topped, or flat), and with or without a central pit [13-16]. Although shields typically occur in clusters (~50-350 km diameter

regions, 100-150 km mode; covering ~10,000 km^2) called shield fields [16], the shields of V-23 do not; rather they describe an extensive morphological unit similar to the shield plains originally described by Aubele [17]. Aubele [17] delineated a morphologic unit, "shield plains," that covers ~2.3 million km^2 and hosts small shields at a density of ~4500/10^6 km^2 within northern Niobe Planitia (V-11, V-12). Aubele proposed that the shield plains unit might extend from 7º N. to 67º N. Indeed this unit occurs across most of V-23 and V-24.

Although some workers believe shields formed during a specific time predating regional plains [18], others propose that shield fields both predate and postdate regional plains [16, 19]. Detailed mapping of seven dispersed regions indicates that shield fields are time transgressive with respect to local regional plains emplacement and deformation [20]. Mapping of local F-tiles in V-23 and V-24 also supports time transgressive shield formation.

Shields across the map area are distinguished based on the characteristics noted above, as well as by quasi-circular to circular regions of relatively homogeneous texture on an otherwise penetratively textured region, interpreted as a region of local volcanic cover on surface marked by a delicate penetrative deformation fabric. Shields are distributed across Niobe, Sogolon and Llorona Planitiae with no discernible patterns at any scale. The shields are not aligned along local fractures, nor are they clustered. What makes these shields so striking is their pervasive distribution across >10x10^6 km^2 across V-23 and V-24.

Shields locally cover--therefore postdate--fractures, wrinkle ridges, or polygonal fabrics, yet they are also locally cut by structures of the same morphology and orientation. The delicate nature and the regionally extensive distribution with little change in orientation of the secondary structures indicate that shield material forms an extremely thin (locally absent) layer. The layer forms a sort of volcanic veil with varying visibility of (underlying) tectonic structures. Shields coalesce into a thin mechanical layer—a shield-paint layer—that is locally deformed by parallel or polygonal wrinkle ridges, or parallel closely spaced extension fractures. The layer also locally records reactivation in which surface fractures filled with 'paint' and later contraction resulted in inversion of the shield paint. Small shields are preserved almost everywhere across the quadrangle except well within the interior of tessera terrain at its highest elevations. Along the edges of the exposed tessera terrain the shields serve to mask or veil the tessera ribbon and fold structures.

V-23 may host as many as 33 impact craters; this number together with a relative lack of impact crater haloes, defines this region as representing an 'old' *average composite surface retention age* [21]. Old and intermediate *average composite surface retention age* provinces display spatial point densities of between 2.73 to 2.53, and 1.45 to 2.53 craters/10^6 km^2, respectively [21]. These data indicate that the surface of V-23 has likely been able to preserve impact craters for quite some time; it does not indicate the absolute or relative age of individual volcanic deposits or morphological features, or the absolute or relative age of various secondary structural suites.

The planitiae across V-23, V-24 and V-25 host a series of north-trending elongate basins and rises with wavelengths of 1000-1500 km. Gravity highs generally correlate with elevated topography, which preserves variably sized ridge belts, tracts of ribbon-bearing tessera terrain [11], and pervasively fractured terrain. Ridge belts trend both NE and NW in V-25 and E V-24; numerous small to large ribbon-bearing tessera terrain occur across V-23 and V-24.

In V-24 and V-23, within southwestern Llorona, Sogolon, and Niobe Planitiae, low circular topographic ridges and radial to concentric fractures mark isolated corona structures, but recognizable long corona-

source flows are rare. Instead an extensive layer of small shields covers the surface. The shields, small (1-15 km diameter) quasi-circular to circular radar-dark or -bright features with or without topographic expression, form a sort of lacey volcanic veil with varying visibility of underlying tectonic structures.

The regional preservation of tessera inliers with coherent structural trends, as well as the coherence and preserved details of delicate, regionally extensive tectonic structures, indicate that the shield paint layer, though developed over some $10x10^6$ km^2, forms a thin discontinuous layer. Detailed mapping of several individual SAR F-tiles shows that shield density is locally >10,000 shields/10^6 km^2 and that shield emplacement was time transgressive with reactivation (or formation) of tectonic structures [22]. Shields represent regionally distributed point-source volcanism. The spacing and size of the shields and their lack of recognizable patterns or trends indicate that melt for individual shields formed at relatively shallow levels across the entire region affected by shields.

The character of V-23 and V-24 contrasts that of V-25 and V-37 where flows sourced from coronae cover much of the plains regions. Channels are also much more common in V-25 and V-37 and may well represent collapsed lava tubes that fed the long coronae-sourced flows. Thus, the northern Aphrodite plains appear to display two very different modes of volcanic resurfacing: by extensive corona-sourced flows to the east (V-25/V-37) and, by a thin volcanic veil comprised of numerous individual shields to the west (V-23/V-24).

References. 1. JE Guest, ER Stofan (1999) *Icarus* 139, 55-66. 2. GG Schaber *and others* (1992) *JGR* 97, 13257-13302). 3. RJ Phillips *and others.* (1992) *JGR* 97, 15923-15948. 4. MA Bullock, GH Grinspoon (2001) *Icarus* 150, 19-37. 5. SC Solomon, MA Bullock, DH Grinspoon (1999) *Sci.* 286, 87. 6. FS Anderson, SE Smrekar (1999) *JGR* 104, 30743-30756. 7. RJ Phillips, VL Hansen (1998) *Sci.* 279, 1492-1497. 8. VL Hansen, HR DeShon (2002) USGS map I-2752. 9. DA Young, VL Hansen (2002), revision to USGS. 10. LF Bleamaster, VL Hansen (2001), submitted to USGS. 11. VL Hansen, JJ Willis (1998) *Icarus* 132, 321-343. 12. HR Deshon (2000) DA Young, VL Hansen, *JGR* 105, 6983-6995. 13. J.C. Aubele, E. N. Slyuta, *EMP* 50/51, 493-532 (1990). 14. J.W. Head, and others, *JGR* 97, 13153-13198 (1992). 15. J.E. Guest and others, *JGR* 97, 15949-15966 (1992). 16. L.S. Crumpler and others, in *Venus II Geology, Geophysics, Atmosphere, and Solar Wind Environment* S.W. Bouger, D.M. Hunten, R.J. Phillips, Eds. (The University of Arizona Press, Tucson, AZ, 1997) pp. 697-756. 17. J.C. Aubele, LPSC XXVII, 48 (1996). 18. A.T. Basilevsky, J.W. Head, *JGR* 103, 8531-8544 (1998). 19. J.E. Guest, E.R. Stofan, *Icarus* 139, 55-66 (1999). 20. E.A. Addington, *Icarus* 149, 16-36 (2001). 21. RJ Phillips, NR Izenberg (1995) *GRL* 22, 1517-1520. 22. V.L. Hansen and others, LPSC, pdf 1061 (2002).

GREENAWAY QUADRANGLE (V-24), VENUS: INITIAL RESULTS

N.P. Lang and V.L. Hansen, Department of Geological Sciences, Southern Methodist University, Dallas, TX 75275 (nlang@mail.smu.edu)

Introduction. The V-24 quadrangle (120°-150° E.; 0°-25° N.) comprises a part of the Aphrodite plains region and displays evidence of volcanic and tectonic processes at many scales. Coronae and small shields source volcanic flows that interact with several tectonic elements of the planitia including broad scale topographic basins, tessera terrain, spaced lineaments, wrinkle ridges, and penetrative fractures resulting in a geologically complex and interesting region.

Methodology. Detailed mapping is being performed using the Magellan 250-meter/pixel and 75-meter/pixel data sets together with synthetic stereo. The mapping philosophy employed here is similar to that outlined by Hansen [1]. Mapping follows USGS guidelines.

Map area and units. Currently, eight major features have been mapped: tessera terrain, Intra-Tessera Basin flows (ITB's), coronae with associated flows, shields with associated flows, pervasively fractured terrain, impact craters with associated materials, lineaments, and wrinkle ridges. Several east- and northeast-trending ridge belts have also been identified across the quadrangle.

Tessera and ITB's. Tessera terrain dominates the western and southern parts of the quadrangle with several isolated inliers found across the plains. Tessera terrain contain both northeast- and northwest-trending sets of structures (fractures and ribbons) as well as northwest- and northeast-trending ITB's filled with volcanic flows apparently sourced, at least in part, from shields.

Tessera terrain contacts with adjacent units are sharp to gradational. Sharp contacts tend to occur in areas of high tessera topography. Gradational contacts occur in areas where tessera terrain appears to grade into a series of kipukas or where tessera terrain related structures (that is, ribbons) extend from the tessera terrain into the adjacent units and appear to be partially covered. Gradational contacts associated with kipukas may possibly be due to corona and/or shield sourced flows flooding low-lying regions of tessera terrain. Reactivation of some tessera structures may be responsible for their continuation from the tessera into adjacent units.

Pervasively fractured terrain. This unit is found predominantly in the eastern part of the quadrangle and is characterized by tightly spaced northwest- to west-striking fractures. Several small inliers of this unit have also been identified across the map area. This unit has a topographically low expression and is commonly embayed by volcanic flows that post-date fracture formation. This unit also appears to have a gradational contact with tessera terrain locally.

Corona and associated flows. V-24 contains seven coronae, which are in the western and central parts of the quadrangle. Each corona is marked by low circular to quasi-circular topographic ridges and/or fractures. Domes (possibly pancake domes?) have been identified around the annuli of several of the coronae.

Large corona flows have been mapped in the southwest (from Rosmerta Corona), in the north (from Boann Corona in V-12), and in the northeast (from Ituana Corona in V-25). Possible flows sourcing from Kamadhenu Corona have been identified but the extent of these flows is obscured due to dark haloes surrounding Marie Celeste, Greenaway, and Callirhoe impact craters to the east. Flows also have been mapped extending from Kubebe Corona, but these flows appear to be relatively localized.

Shields and associated flows. Shields are identified as low circular to quasi-circular mounds that may have a summit pit. Shields are by far the most abundant feature in the quadrangle; shields are not limited to shield fields.

Flows, as observed in high-resolution SAR images, have been identified and mapped extending from these shields. Shield flows are small and localized and are commonly difficult to delineate because they typically appear to coalesce with flows from adjacent shields.

Impact craters and associated materials. Seventeen impact craters have been identified and mapped across V-24. All craters have a raised rim and visible ejecta blanket. Some ejecta materials extend for over a hundred kilometers from the rim. Most craters also contain a dark floor and a central peak. Dark haloes have been identified surrounding most of the impact craters. Only a few of the impacts show clear evidence of tectonism.

Wrinkle ridges. Wrinkle ridges occur across the entire quadrangle, typically with an east to northeast trend.

Lineaments. Lineaments representing predominantly faults and/or fractures are also found across the entire quadrangle. These features display regionally consistent patterns defined by north-northwest to north-northeast strike.

Summary. Volcanic flows sourced from coronae and shields have interacted with an array of tectonic features in V-24 resulting in a geologically complex region. Stratigraphically, tessera terrain and the pervasively fractured terrain appear to be the locally oldest units in the quadrangle, although their relative age to each other is unknown. Other units that lack distinctive deformation features could also be equally old, or older than either of these units. Structural elements within both the tessera terrain and the fractured terrain appear to have been locally reactivated following deposition of younger units. All other units appear to post-date the tectonism of the tessera terrain and pervasively fractured terrain, but the relative ages of these units are difficult to determine from these initial results and warrants more detailed mapping.

References. [1] Hansen, V.L. (2000), Earth and Planetary Science Letters, 176, 527-542.

MAPPING OF VENUS QUADRANGLES V-46, V-28, V-53, V-30, AND V-39.

Ellen Stofan[1, 2], John Guest[2] and Antony Brian[2]. [1]Proxemy Research, 20528 Farcroft Lane, Laytonsville MD 20882; [2]Department of Geological Sciences, University College London WC1E 6BT UK; ellen@proxemy.com

We have recently resubmitted final revisions from map editor comments for quadrangle V-46, which has now been accepted. V-39 has been submitted for review (as of 6/27/02), and we are in the process of transferring final maps of quadrangles V-53, V-30 (D. Crown), and V-28 into digital form for submission. We are now integrating our analysis of these quadrangles with results from mapping by Guest and others of quadrangles V-19, V-31, and V-33. V-33 is being revised according to reviewer comments; V-31 was also submitted 6/27/02. V-19 is being transferred into digital form.

Our quadrangles can be found in three basic settings: plains, chasma/fracture belts, and volcanic rises. V-33 and V-19 are located in the plains; V-46, V-53, V-39, and V-28 along chasma/fracture belts, and V-30 and V-31 at volcanic rises. In most of the regions we have mapped, the plains are a patchwork of smaller-scale (10's to 100's km^2) resurfacing. Most of our regional-scale plains are cut by one to three sets of wrinkle ridges. In most cases, the wrinkle ridges are not distributed uniformly within a plains unit, with some parts of the unit remaining undeformed. All of the wrinkle ridges appear to have formed in response to local to regional-scale tectonics.

Chasma Regions. Our quadrangles are located along Juno Chasma and Hecate Chasma, and two along Parga Chasma. In these regions, rifting and faulting deformed the plains, with extensive volcanism from coronae and volcanoes along and adjacent to the chasmata. The plains surrounding the chasmata are distinct from the plains units in other regions that we have mapped, in that they contain a very high concentration of small volcanic edifices. As in other plains units that we have mapped, the small edifices appear to have a range in age relative to their 'host' unit, with some younger than the background plains and others embayed by them.

Volcanic Rises. Our quadrangles cover two volcanic rises: western Eistla Regio and Laufey Regio. Lava flows from coronae and volcanoes at these rises superpose the surrounding plains units, but we think it likely that plains flows and rise flows are interfingered (for example, Guest and Stofan, 1999). In general, wrinkle ridges do not cut the flank flows from the volcanoes. Exceptions to this are seen at Gula Mons and Var Mons, where some older flow units are deformed by wrinkle ridges [Brian and others, 2002; Stofan and others, 2001].

Plains Regions. One of our quadrangles is in Tinatin Planitia and another in Sedna Planitia. These areas are dominated by several types of plains units, from more sheetlike plains to those composed of multiple smaller flows. In these regions, the bulk of the plains cannot be associated with a specific source.

Initial Results. In each quadrangle, we classified surface areas as corona-related flows, rift-related flows; edifice fields, flows associated with edifices 10-100 km in diameter, flows associated with edifices >100 km in diameter; plains/flows with no identifiable source; structure or craters; or data gaps. We have assessed the percentage area of each of these types of areas in each of our quadrangles, in order to better understand the sources, scales, and timing of volcanic resurfacing.

Our initial analysis of resurfacing styles and scales indicates that large volcanoes and coronae are significant sources of resurfacing at volcanic rises, while coronae and edifice fields dominate along chasmata. Multiple sources are responsible for resurfacing, with rift-related flows the most insignificant, even along chasmata. Resurfacing has occurred at scales from 10's to 1000's of km^2. The bulk of volcanic

terrain in each quadrangle could be tied to a specific volcanic source.

We have found that different types of regions on Venus have distinct differences in the sources and scales of resurfacing. These results will be used, along with stratigraphic information, to help constrain models of the evolution of the Venus surface. When combined with our mapping, this analysis suggests that resurfacing has occurred throughout the mappable history of these regions. We are in the process of relating this work to broader scale models of Venus resurfacing (for example, Bullock and Grinspoon, 2001).

References. Brian, A.W., E.R. Stofan, J.E. Guest and S.E. Smrekar, Laufey Regio: A new topographic rise on Venus, submitted, 2002.; Bullock, M.A. and D.H. Grinspoon, The recent evolution of climate on Venus, Icarus, 150, 19-37, 2001.; Guest, J.E. and E.R. Stofan, A new view of the stratigraphic history of Venus, Icarus, 139, 55-66, 1999.; Stofan, E.R., J.E. Guest and D.L. Copp, Development of large volcanoes on Venus: Constraints from Sif, Gula and Kunapipi Montes, Icarus, 152, 75-85, 2001.

TECTONIC AND VOLCANIC HISTORY OF THE NEPTHYS MONS QUADRANGLE (V-54), VENUS

Nathan T. Bridges, Jet Propulsion Laboratory, California Institute of Technology (MS 183-501, 4800 Oak Grove Dr., Pasadena, CA 91109; nathan.bridges@jpl.nasa.gov)

Introduction. Mapping of Venus' Nepthys Mons quadrangle (V-54, 300-330° E., 25-50° S.) has been proceeding for the last 26 months. Major research areas addressed are how the styles of volcanism and tectonism have changed with time, the evolution of shield volcanoes, the evolution of coronae, the characteristics of plains volcanism, and what these observations tell us about the general geologic history of Venus. Recent mapping has been significantly augmented by the use of pseudostereo anaglyphs made from left and right pseudostereo pairs for Cycle 1, 2, and 3 images. The advent of this great data set has revised many of the mapping interpretations reported previously [1,2]. Discussed here are several intriguing findings.

Methods. Mapping for this project has proceeded in several stages. First, geologic units and structures were mapped on hardcopy USGS FMAP's and then transferred to the 1:5 million-scale map base. Pseudostereo anaglyphs were produced by placing left-right stereo pairs into red and blue channels and combining these into an RGB file. These products have proven an indispensable tool and have resulted in a virtual complete revision of previously mapped areas [1,2]. At FMAP scale, structural trends and inferred ages were broken out using different symbols and colors. These will eventually be transferred to a 1:5 million-scale structure map separate from the geologic map. The geologic units, structures, impact craters, coronae, and volcanoes are being arranged in time-stratigraphic sequences as the mapping progresses. Both computer-based and traditional paper/pencil mapping techniques have been implemented as the PI gains experience with the latter. Presented at this meeting will be an unfortunate mishmash of both. If funded, future mapping efforts have proposed to use GIS techniques.

General Stratigraphy and Structure. Using basic geologic mapping principles [3], 33 units have been broken out, consisting of flow materials (11 units), volcanic construct materials (5 units), plains materials (12 units), tessera material (1 unit, with considerable structural variability), and impact crater materials (4 units; fig. 1). Tessera, distributed as scattered inliers, appears to be the oldest unit and is truncated by tectonized plains and other plains units. Stratigraphically above these regional plains units are scattered fields of shields and associated flows. Polygonal flows are common and appear to show a range of ages. Flows associated with coronae and shield volcanoes are intermediate to young in age. For all cases, craters appear to be younger than adjacent units, consistent with other areas on Venus [4]. No craters have been found on the large shields.

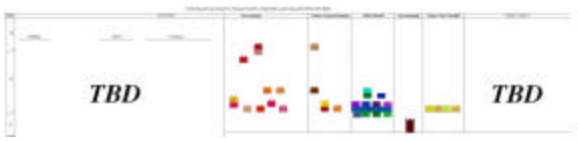

Figure 1. Correlation chart for quadrangle V-54.

Interesting Results and Observations. Tessera—To better understand the complex structural relationships within tesserae, I have mapped out individual structural trends and attempted to estimate the history of activation for these mapped sets, following in many respects efforts of previous workers [5]. An example is shown in figure 2. Here, a NE-SW set of lineaments, shown as blue lines, are cross cut by the other structures, are generally confined to the tessera region, and do not extend past the tessera-adjacent textured plains material (unit ptt shown in green). Later, extensional stress caused the

formation of the N-S grabens (shown as yellow lines). They too are mostly confined to the tessera region and do not extend past unit ptt. At some point after these two families of structures formed, the region was volcanically flooded and parts of the structures were covered. This gave rise to unit ptt to the south and east of the main tessera block. Formation of these structures may have continued after the flooding, but it is difficult to distinguish between structures that formed before the flooding, but were not covered, and those that may have formed after the flooding. Next there was uplifting of the tessera region and then the regional plains member 2 (unit pr_2 shown in light blue) embayed the tessera and unit ptt. Note that neither the NE-SW nor the N-S structures are found in unit pr_2, so their formation must have been completed by the time unit pr_2 existed. The last set of structures to form, the WNW-ESE grabens (shown as red lines), were caused by extensional stresses that probably began after unit ptt emplacement and ended later in the sequence after the formation of unit pr_2. Note that they appear to cross cut the other two structure sets, and some of them appear to stop at the ptt/pr_2 boundary, leading to the conclusion that some of these grabens must have formed before unit pr_2.

Such detailed analyses are being conducted for each mappable tessera outcrop, after which a comparison of these results will be made to previously proposed models for tesserae [6-10].

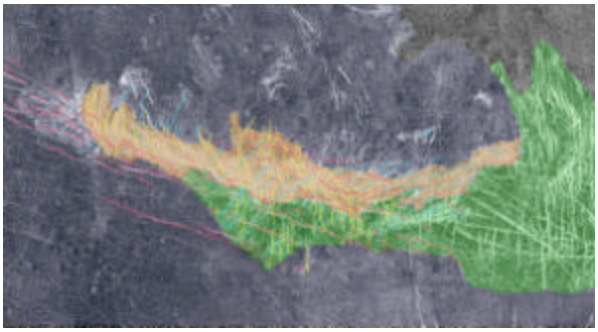

Figure 2. Mapped tessera block in V-54. See text for details.

Polygonal and Shield Plains—Polygonal plains are now mapped as a single unit of intermediate age (as opposed to three previously [1,2]), but several members with locally distinct stratigraphic position are apparent. Shield-rich plains are intermediate to young, consistent with observations in some quadrangles [11,12] and inconsistent with others [13,14] (that is, small shields form throughout the geologic history of Venus). The polygonal plains are commonly associated with and, in many cases, difficult to distinguish from, shield plains (fig. 3). This suggests that the polygons are lava flow cooling structures, as opposed to the manifestation of cooling stresses from planet-wide global change [15-17]. However, the polygons are enigmatic features that are still poorly understood and we are open to other interpretations as the mapping progresses.

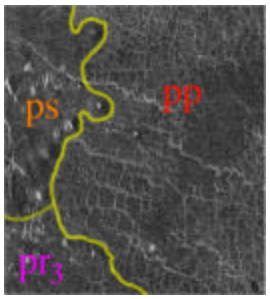

Figure 3. Contact among polygonal plains (pp), shield plains (ps), and member 3 of the regional plains (pr_3).

Large shield volcanoes and coronae—One of the original goals of this mapping effort was to find stratigraphic relationships among coronae, large shield volcanoes, and intermediate structures. Many of the relationships are quite complex, requiring detailed structural mapping such as that described for the tessera above. Many shields (for example, Tefnut Mons) have corona-like radial structures and there is commonly no obvious distinction between feature names “corona,” "mons," and “patera.” The flows from these features can be mapped out and in some cases stratigraphic relationships determined; in other examples, this is more difficult (fig. 4). Large flows from shields/coronae commonly

post-date regional plains and many local structures.

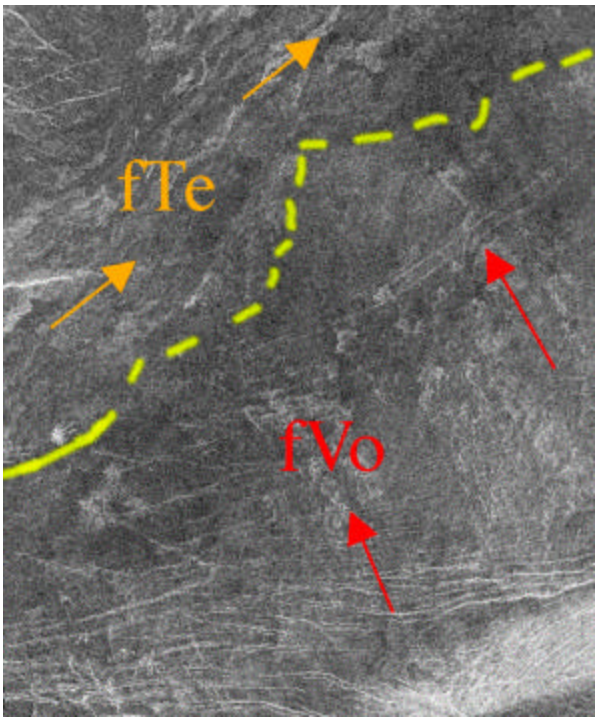

Figure 4. Dashed contact between flows of Tefnut Mons (fTE) and the outer flow member of Vovchok Patera flow material (fVo). Although stratigraphic relationships here are equivocal, mapping elsewhere in the quadrangle shows that unit fVo post-dates most of the fTe flows.

Acknowledgments. I am indebted to the mapping assistance of C.M. Mercer (Oberlin College) during the summer of 2001. She was supported under the Planetary Geology and Geophysics Undergraduate Research Program.

References. [1] Bridges, N.T. (2001), Lun. Plan. Sci. XXXII, 1376. [2] Bridges, N.T. (2001), Planetary Mappers' Meeting, Albuquerque, NM. [3] Wilhelms, D.E. (1972). Geologic Mapping of the Second Planet, Interagency Report: Astrogeology 55, U.S. Geological Survey. [4] Schaber, G.G. and others (1992), JGR, 97, 13,257-13,301. [5] Hansen, V.L. (2000), Earth Plan. Sci. Lett., 176, 527-542. [6] Bindschadler, D.L. and Head, J.W. (1991), JGR, 96, 1523-1554. [7] Bindschadler, D.L. and others (1992), JGR, 97, 13,495-13,532. [8] Hansen, V.L. and Willis, J.J. (1996), Icarus, 123, 296-312. [9] Ivanov, M.A. and Head, J.W. (1996), JGR, 101, 14,861-14,908. [10] Gilmore, M.S. and others (1998), JGR, 103, 16,813-16,840, 1998. [11] Aubele, J.C. (1996), LPSC XXVII, 49-50. [12] Basilevsky, A.T. and J.W. Head (1998), JGR, 103, 8531-8544. [13] Addington, E.A. (1999), LPSC XXX, 1281. [14] Guest, J.E. and E.R. Stofan (1999), Icarus, 139, 55-66. [15] Bullock, M.A. and D.H. Grinspoon (1996), JGR, 101, 7521-7529. [16] Solomon, S.C. and others (1999), Science, 286, 87-90. [17] Anderson, F.S. and S.E. Smrekar (1999), JGR, 104, 30,743-30,756.

GEOLOGIC HISTORY OF LADA TERRA, VENUS: ASSESSMENT FROM PRELIMINARY MAPPING OF MYLITTA FLUCTUS QUADRANGLE (V-61) AND LADA TERRA QUADRANGLE (V-56)

M.A. Ivanov[1,2] and J.W. Head[2]. [1]Vernadsky Institute, RAS, Moscow, Russia, mishaivn@mtu-net.ru; [2]Brown University, Providence, RI, USA, james_head_iii@brown.edu

Introduction. Lada Terra is a large (from 300° E. to 120° E. and from 60° S. to 80° S.) elevated region on Venus. It is characterized by a wide variety of features, among which coronae play the most important role. The western portion of Lada Terra is dominated by the very large (~800 km), Quetzalpetlatl Corona [1,2], and smaller coronae typically arranged in linear zones characterize the rest of this topographic province. To the northwest and northeast, the lowlands of Lavinia and Aino Planitiae border Lada Terra. The two quadrangles, V-61 and V-56, cover the western and central portions of Lada Terra and the whole structure of Quetzalpetlatl Corona, show the transition from Lada Terra to the surrounding lowlands, and display the major structural trends at the edges and in the interior of Lada Terra. During our mapping in the V-61 area and reconnaissance mapping within V-56 quadrangle we have analyzed the nature and age of the topographically highest large corona (Quetzalpetlatl) and documented the most prominent structural trends, their nature, and timing.

Area of V-61 quadrangle (Fig. 1a). The most spectacular feature of this quadrangle is Quetzalpetlatl Corona, represented there by its western half. The structurally most prominent part of the corona is its annulus, consisting of densely spaced ridges up to 10 km wide. The ridges make up an arclike belt outlining the northern and northwestern sectors of the corona. A topographic moat partly filled with lava is adjacent to the belt on its outward side and there is no counterpart to the ridge belt/moat complex in the southern portion of Quetzalpetlatl. The corona is also a large volcanic center and relatively young lava flows cover the internal part of Quetzalpetlatl and the vast area around it. The sources of the flows appear to be close to the center of Quetzalpetlatl (Boala Corona and a longitudinally oriented swarm of grabens that runs from Boala toward the northern edge of Quetzalpetlatl).

Several distinct structural trends characterize the area within V-61 quadrangle. In the lowlands of Lavinia and Helen Planitiae, several continuous topographic ridges (Morrigan Linea, Penardun Linea, etc.) separate the vast lowlands into a series of secondary basins [3-5]. Morphologically, these zones consist mostly of ridge belts and relatively old units broadly embayed by regional plains. The Kalaipahoa Linea that represents a swarm of grabens and hosts two coronae, Kamui-Huci in the west and Jord in the east, introduces another structural trend. Kalaipahoa Linea makes a broad arc that topographically corresponds to the edge of Lada Terra. The grabens of Kalaipahoa Linea cut regional plains and appear to be partly contemporaneous with the younger lava flows emanating from Quetzalpetlatl. Jord Corona and Tarbell Patera adjacent to it are the sources of the gigantic Mylitta Fluctus [6] that flows down the regional slope into the lowland of Lavinia Planitia.

Area of V-56 quadrangle (Fig. 1b). The western portion of this area is characterized by the eastern half of Quetzalpetlatl Corona that bears the same basic characteristics as in the V-61 quadrangle. The ridge belt/moat complex outlines the northern portion of the corona and has no counterpart in its southern part. The vast apron of young lava flows covers the regional slopes away from the corona. The apparent sources of the flows are Erzulie Mons and a cluster of small shields in the southeastern sector of Quetzalpetlatl.

The main difference of the V-56 area from the V-61 quadrangle is that it contains

two large massifs of tessera terrain (Cocomama and Lhamo Tesserae). These tesserae appear to be the oldest terrain in the scene and establish the oldest structural trends in the quadrangle. Cocomama Tessera dominates the central portion of Lada Terra, and the Lhamo Tessera is a part of a regional highland ridge that borders the eastern edge of Lavinia Planitia [7]. In the northeastern corner of the quadrangle, within the lowland of Aino Planitia, a double forklike topographic ridge consists of Asiaq and Kuldurok Dorsa. This ridge is made up of ridge belts and is broadly embayed by regional plains. By its topographic, morphologic, and stratigraphic characteristics the Asiaq and Kuldurok Dorsa belt strongly resembles the old structural zones occurring in the V-61 quadrangle within the lowlands surrounding Lada Terra.

Two very prominent young structural zones characterize the V-56 area. The first occurs in the northwestern corner of the area and is a continuation of the Kalaipahoa Linea. The most important feature of this zone within the V-56 quadrangle is Eithinoha Corona (~400 km). The swarms of grabens that characterize the Kalaipahoa Linea structural zone run along the edge of Lada Terra and cut through Lhamo Tessera, suggesting the superposition of the older and younger zones in one area. The second large zone is in the central portion of the quadrangle. It is oriented longitudinally and consists of a chain of relatively small coronae interconnected by swarms of grabens. This zone is split into three branches at about 65° S., 40 ° N. The most prominent, western, branch, which is characterized by large (~350 km) Otygen Corona, merges with the Kalaipahoa Linea in the northwestern corner of the quadrangle. The central branch apparently dies out at the northern edge of Lada Terra and the eastern branch runs into the eastern portion of it (out of the V-56 area).

Summary. Our analysis of the two neighboring quadrangles reveals preliminary evidence for the progressive change of volcanic and tectonic styles as a function of time at regional scale within Lada Terra. Cocomama Tessera, which is heavily embayed by all types of volcanic plains and occurs in the center of Lada Terra, may represent an outcrop of the ancient basement of this region. The relatively older structural zones that are embayed by regional plains and represented mostly by the ridge belts (for example, Morrigan Linea, Kuldurok Dorsa, etc.) are restricted within the lowlands and rarely occur within the highland of Lada Terra. Quetzalpetlatl Corona may represent a long-lived structure if its northern rim is a fragment of a ridge belt. The rim, however, may be due to internal corona evolution, which is suggested by the spatial association of it with the moat. This kind of association commonly occurs at a number of large coronae [8-10]. The youngest structural trends represented by the corona-rift zones occur within the elevated Lada Terra region [11]. In contrast to the older zones, the corona-rift chains do not extend into the lowlands, are absolutely dominated by extensional structures, and the sources of young vast lava flows typically occur along these zones.

References. [1] Stofan, E.R., and others, JGR, 97, 13347-13378, 1992. [2] Stofan, E.R., and others, Coronae on Venus: Morphology and origin, in Venus II Geology, Geophysics, Atmosphere, and Solar wind environment, S.W.Bougher, D.M. Hunten, and R.J. Phillips eds., Univ. Arizona Press Tucson, 931-965, 1997. [3] Squyres, S.W., and others, JGR, 97, 13579-13599, 1992. [4] Banerdt W.B., and others, Plains tectonics on Venus, in Venus II Geology, Geophysics, Atmosphere, and Solar wind environment, S.W.Bougher, D.M. Hunten, and R.J. Phillips eds., Univ. Arizona Press Tucson, 901-930, 1997. [5] Ivanov, M.A. and J.W. Head, Geologic map of the Lavinia Planitia (V-55) quadrangle USGS Geol. Inv. Ser., Map I-2684, 2001. [6] Roberts, K.M., and others, JGR, 97, 15991-16016, 1992. [7] McGill, G. and N. Bridges, Geologic map of the Kaiwan Fluctus Quadrangle (V-44),

Venus, USGS, Geologic Investigation Series, Map I-2747, Scale 1:5,000,000, 2002. [8] Janes, D.M. and S.W. Squyres, JGR, 100, 21173-21187, 1995. [9] Schubert, G. and T.D. Sandwell, Icarus, 117, 173-196, 1995. [10] Ivanov, M. A. and J. W. Head, Geologic map of the Atalanta Planitia (V-44) quadrangle USGS Geol. Inv. Ser., in edit 2002. [11] Magee, K.P. and J.W. Head, JGR, 100, 1527-1552, 1995.

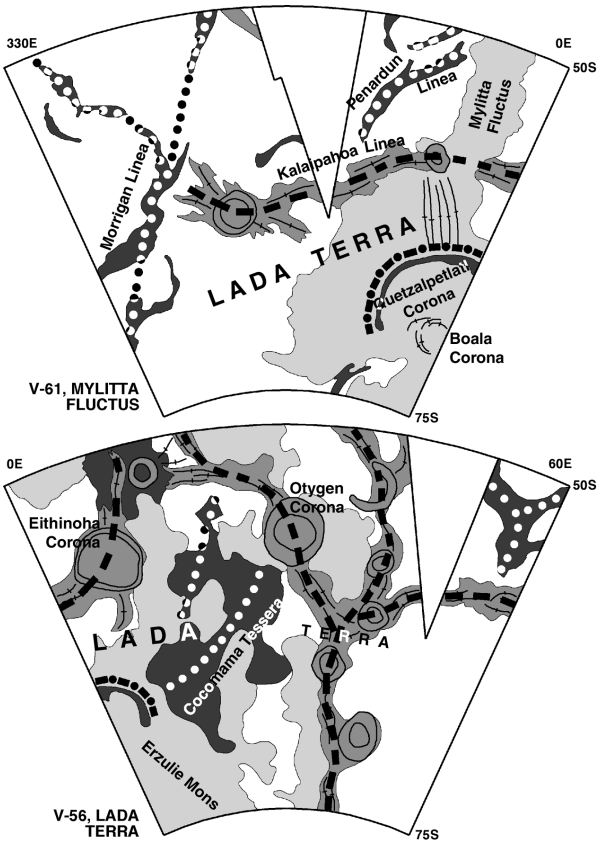

Figure 1. Sketch maps of V-61 and V-56 quadrangles. Dark gray indicates older structural zones, young corona-rift zones are shown in gray, and light gray shows young lava flows. Strikes of structural trends are shown in dotted (old) and dashed (young) lines.

GLOBAL GEOLOGIC MAPPING OF EUROPA: CONSIDERATIONS FOR FUTURE EXPLORATION

P. Figueredo[1], R. Greeley[1], K. Tanaka[2], and D. Senske[3]: [1]Arizona State University; [2]U.S.G.S., Flagstaff; [3]NASA headquarters – figueredo@asu.edu

Introduction. As outlined by Greeley and Carr [1], the significance of any event on a planetary surface is clearest if viewed in its historical context. In addition, chemical and physical analyses can be planned and interpreted far better if the geologic setting of the place of measurement is known; without such knowledge, chemical and physical measurements can be misleading. Geologic frameworks are based on understanding the stratigraphy and structural geology of the units and features exposed on planetary surfaces, as determined through geologic mapping. Geologic mapping reduces the complexity of a planetary surface by dividing the near-surface materials into units and mapping their distribution [1-5]. Geologic units must then be interpreted in light of the internal and external geologic processes that resulted in their present configuration, and stratigraphic studies will indicate the time relations between them.

Europa mapping. Lucchitta and Soderblom [6] produced the first terrain map of Europa from Voyager images of the trailing hemisphere. Galileo increased significantly the coverage and resolution of Europa imagery, and geologic maps were produced from these new data at a variety of scales [7-13]. The most extensive geologic mapping from Galileo data consists of two pole-to-pole maps across the leading and trailing-antijovian hemispheres of Europa [14, 15]. Greeley and others [16] presented guidelines for the geologic mapping of Europa and characterized many of the major units, subunits, and structures; in addition, they proposed a system of nomenclature, symbols, and color conventions. Five primary units were defined from Galileo images of Europa: plains, chaos, band, ridge, and crater-related materials [16]. The plains material resulted from a complex history of early tectonic and cryovolcanic events that produced a heavily modified background unit. Chaos material comprises areas of disruption, reworking, and partial replacement of preexisting units by subsurface activity. Band materials form wide linear features that resulted from relative motions between icy crustal plates. Ridge material resulted from the buildup of material derived from an initial fracture. Crater materials include those associated with impact features, such as ejecta deposits.

Emerging geologic history. The geologic histories derived from Europa maps generally indicate early formation and modification of background plains, subsequent cross-cutting and emplacement of an intricate network of bands and ridges, followed by chaotic disruption of the surface [8-10, 14, 15]. To date, there has been no attempt to correlate these local or regional relationships into a global stratigraphic record. The mentioned sequence reveals a possible gradual change in the style of resurfacing with time, from tectonic- to cryovolcanic-dominated processes [for example, 15, 17, 18]. One plausible mechanism for this change is the gradual thickening of Europa's lithosphere to the stage at which solid-state convection was initiated [17, 19]. Current geologic mapping has documented narrowing of bands and an increase in lineament spacing with time, as well as recent diapiric upwellings originating tens of kilometers deep in the ice [15, 20]. These elements suggest an increasing difficulty in fracturing and separation of crustal plates with time, consistent with local crustal thickening with time. However, it remains to be determined whether this trend occurs on a global scale. In this sense, evidence for thickening derived from global geologic mapping has the potential to reconcile models that are currently under intense debate, as lithospheric thickening could indicate a transition between

proposed thin-shell and thick-shell models of Europa (reviewed by [21, 22]).

Importance of global geologic mapping. Determining the sequence of events involved in the evolution of planetary surfaces leads to the establishment of generalized geologic time scales, that is, frameworks for placing rock units into relative ages in which one unit is older or younger than another unit. To do that, we intend to produce the first global geologic map of Europa.

Contact relationships documented on current regional geologic maps [e.g., 8-10, 14, 15] will be extrapolated to global scales to enable the use of major lineaments as stratigraphic markers. We intend to determine the stratigraphic position of each major lineament (or group of lineaments) that collectively comprise the global network, allowing the bracketing between lineaments of any event or occurrence through the geologic record. The network of dated lineaments has the potential to correlate geologic histories derived from different areas and will constitute a framework within which to reference existing and future maps. In the absence of a well-developed cratering record, this alternative stratigraphic reference will contribute to the understanding of the geologic evolution of Europa; in fact, this could turn out to be the only approach for establishing a geologic time scale. Still, our geologic map will show the distribution of impact craters on a global scale [compare with 23], placing these areas into a global geologic context. With a global stratigraphic perspective, we will link events and show the occurrence of processes at specific or different places and times. In this way we plan to synthesize the global geologic history of Europa.

Considerations for future exploration. A global geologic map of Europa will provide a geologic context for mapping of other Galileo observations of Europa at regional and local scales and will reveal areas for further targeting on future missions to Europa. In addition, it can lead to the identification of areas where the cross-cutting relations of key lineaments remain unclear, and that should be targeted on future missions in order to connect regional stratigraphies.

Determining the location and distribution of units associated with tectonic and cryovolcanic processes that may have emplaced materials from the underlying ice or liquid water ocean on the surface, and vice versa, has direct implications for the ongoing investigation of the astrobiological potential of Europa [for example, 24, 25]. Areas where surface-subsurface exchanges could have occurred will be likely high-priority targets for future investigations by orbiters and landers [12]. In this sense, the emerging geologic history of Europa indicates that areas of recent or ongoing activity, if any, are likely associated to crustal disruption rather than ridge/band building.

References. [1] Greeley and Carr, eds., NASA SP-417: 13-32, 1976; [2] Carr and others, NASA-SP 469, 1984.; [3] Wilhelms, in Planetary Mapping: 208, 1990; [4] Tanaka and others, U.S. Geol. Surv. Open File Rep., 94-438, 1994; [5] Hansen, Earth and Planet. Sci. Lett., 176: 527, 2000; [6] Lucchitta and Soderblom, in The Satellites of Jupiter: 521, 1982; [7] Senske and others, LPSC XXIX, #1743, 1998; [8] Prockter and others, JGR., 104: 16531, 1999; [9] Kadel and others, JGR., 105: 22657, 2000; [10] Figueredo and Greeley, JGR, 105: 22,629, 2000; [11] Klemaszewski and others, LPSC XXX, #1680, 1999; [12] Prockter and Schenk, LPSC XXXIII, #1732, 2002; [13] Kattenhorn, Nonsynchronous rotation evidence and fracture history in the Bright Plains region, Europa, Icarus, in press; [14] Figueredo and others, Eos Trans. AGU, 81, 48, P72A-17, 2000; [15] Figueredo and Greeley, LPSC XXXIII, #1068, 2002; [16] Greeley and others, JGR, 105: 22,559, 2000; [17] Pappalardo and others, Nature, 391: 365, 1998; [18] Spaun and Head, JGR, 106: 7567, 2001; [19] McKinnon, GRL, 26: 951, 1999; [20] Figueredo and others, Geology and origin of Europa's "Mitten" feature (Murias Chaos),

JGR, in press; [21] Greenberg and others, LPSC. XXXII, #1428, 2001; [22] Pappalardo and Head, LPSC XXXII, #1866, 2001; [23] Turtle and Pierazzo, Science, 294: 1326, 2001; [24] Reynolds and others, Icarus, 56: 246, 1983; [25] Greenberg and others, JGR, 105: 17551, 2000.

GLOBAL MAPPING OF GANYMEDE: GALILEO-RELATED VIEWS OF STRUCTURES, STRUCTURAL RELATIONSHIPS, AND STRUCTURAL UNITS

James W. Head[1], Geoffrey C. Collins[2], and Robert T. Pappalardo[3], [1]Department of Geological Sciences, Brown University, Providence, RI 02912 USA (james_head@brown.edu); [2] Wheaton College, Norton MA 02766. [3]LASP, University of Colorado, Boulder, CO 80309.

Introduction. A significant area of the surface of Ganymede is characterized by light grooved terrain, regions that are relatively high albedo but contain a host of linear features which are commonly parallel, but often arranged in tangentially and orthogonally oriented domains [1]. These features are commonly interpreted as tectonic in origin and have been used by Voyager mappers to define geologic units and structural domains [2].

In principle, geologic map units are material units and should be independent of structure [3], and most workers adopt this approach. In planetary mapping, however, exceptions have often been made due to the local and regional dominance of structural features, the synoptic and remote sensing aspect of the data, and the scale of the mapping [4,5]. On Earth, rock-stratigraphic units are defined as "...a subdivision of the rocks in the Earth's crust distinguished and delimited on the basis of ....observable physical features.. [commonly lithologic]... and independent from time concepts... and.. inferred geologic history..." [3]. In planetary mapping stratigraphic units must be defined largely by remote sensing and so it is difficult to approach the process of geologic mapping of planetary crusts with a strict 'lithologic' definition of units. As outlined by Wilhelms [4,5], planetary mappers use the broader definition of rock-stratigraphic units as those "distinguished and delimited on the basis of observable physical features", which might include surface morphology, albedo, etc. (see also [6]).

Published global geologic maps for the planet Mars at a scale of 1:15 million [7] provide some perspective and precedent for unit definition and characterization on Ganymede. First, in terms of description of map units [7], "although the origin and composition of many units are obscure or controversial, their interpretations are based on objective descriptions of morphologic characteristics visible on ...photomosaics and images." In addition to surface roughness and albedo, a wide range of morphologic structures and textures is utilized to define, distinguish, and characterize units, including crater densities, tectonic fractures, flow lobes, channels, eolian pits, tectonic ridges, and mountain ranges such as crater and basin rims. For example, the grooved member of the Vastitas Borealis Formation is defined by "curvilinear and polygonal patterns of grooves and troughs," whereas the ridged member is characterized by a "concentric pattern of low, narrow ridges about 1 to 2 km wide." The four aureole members of the Olympus Mons Formation are defined as "broad, semicircular, flat lobes; corrugated, cut by numerous faults that formed scarps and deep troughs and grabens." The ridged unit is defined by "long, linear to sinuous mare-type (wrinkle) ridges." Finally, structural deformation plays a large role in the definition of a major geologic unit known as highly deformed terrain materials, where "the origin and composition of these rock units are only surmised because multiple sets of fractures and grabens have obscured original characteristics."

In addition to morphologic features and structures forming an integral part of the definition of geologic map units on Mars, large or prominent such features (faults, graben, wrinkle ridges, sinuous channels, depressions, etc.) are sometimes mapped individually at this scale [7]. Indeed, the distinction and individual mapping of such features, or their inclusion in the definition of a unit, is clearly a function of the scale of mapping. What might be mapped separately as individual structures at a scale of 1:100,000 would very likely be included as

part of a unit definition or characterization at a scale of 1:15M.

On Ganymede, Shoemaker and others [8] defined the grooved terrain as a major geologic unit and considered it "both lithologically and structurally distinct from the ancient cratered terrain." In addition, they mapped additional structural units within it where "each line is the boundary of a structural cell that contains a unified structural pattern." Later workers in the 1:5M-scale geologic mapping program, such as Lucchitta and others [2], found that the "surface of Ganymede seems to be dominated by units of similar compositions but diverse structural patterns," and as discussed above, they point out that "many map units are subdivided mainly on the basis of structural differences..." and that "...locally the structural deformation may have been so intense or pervasive that it created a new and distinct material, distinguished from the parent material by a different physical state rather than a different composition."

The use of structure, even in the qualified manner extensively described above, has raised considerable controversy [9], and this issue needs to be addressed before the final selection of map units and nomenclature is made. This then raises the question, should these features be mapped as structures only, should they be mapped as geologic units, or is there some combination of approaches that is appropriate, perhaps depending on scale? In our presentation we will marshall the arguments pro and con for different approaches for discussion at the mapping workshop.

Secondly, we are producing an update on the geologic relationships and interpretation of the sequence of events in grooved terrain on the basis of the new Galileo data [10], and assessing the global distribution of different structural types [11,12]. In structural and stratigraphic mapping using Voyager data, particular conventions were often developed concerning the relationships of structural features, and these led to a specific interpreted sequence of events [13, 14].

For example, Golombek and Allison [13] proposed a stratigraphic sequence for the formation of grooved terrain in Uruk Sulcus in which they interpret many of the boundaries between groove sets as T terminations of faults, where the younger faults (the stems of the T's) terminate against the structural discontinuity at the older set of faults (the crossbar of the T). Golombek and Allison [13] then used these interpreted stratigraphic relationships to propose a three-stage process of formation for the grooved terrain: (1) initial fracturing of the dark terrain by long primary grooves, (2) secondary grooves link primary grooves and divide the terrain into mechanically isolated polygons, (3) polygons are cryovolcanically resurfaced by bright material, and short tertiary grooves form within the polygons, terminating against the previously formed primary and secondary grooves. Murchie and others [14] proposed a variation on this theme, in which groove lanes are young structures which cut across the polygons (see discussion in [10]). Both hypotheses make different but specific predictions about the nature of the groove lanes at high resolution.

Using the high-resolution views of grooved terrain from Galileo, these hypotheses have been tested. Collins and others [10] found that grooved polygons are the oldest features, not the youngest as predicted by the Golombek and Allison [13] model. They found that different orientations of groove lanes formed sequentially as a function of time and that succeeding groove lanes isolated previous lanes into separated segments and polygons (see their figure 8). The resulting stratigraphic sequence could be mapped over an area of 1.6 million square kilometers, from northwest Uruk Sulcus to Philus Sulcus. The results showed that groove orientations are consistent across large areas within each stratigraphic interval and that grooved polygons could be reconstructed and connected on the basis of these relationships.

These encouraging results meant that the new high-resolution data had provided additional insight into the stratigraphic relationships and sequence of events and that bright terrain structures and stratigraphy could be potentially recognized and mapped at the global scale. These results then provided the incentive to develop the next step, which was to compile a global map of all of the structures on Ganymede using the new global Voyager-Galileo base map image mosaic (a Global Information System, GIS, database). Using Arc/Info GIS software, Collins [11,12] constructed a global database that included virtually every groove, furrow, and dark terrain polygon visible on the surface of Ganymede. He found that there were about 500 polygons of dark terrain comprising about 35% of the surface of Ganymede. Over 61,000 grooves and 4,400 furrows were mapped in GIS and their lengths and orientations computed. The influence of image resolution and viewing geometry (for example, emission angle, incidence angle, and phase angle effects) were carefully assessed.

The analysis of these data from the standpoint of quantitative assessment of structure orientation, spacing, and sequence is the subject of several separate analyses that are underway. These new data provide, however, a unique opportunity to contribute to the geologic map of Ganymede at 1:15M scale. The new sets of groove and furrow locations and orientations (in the updated GIS reference coordinate system) are being combined with the updated geologic unit map. We will present several options including: (1) defining polygon boundaries based on groove terminations and generalizing the individual grooves into average orientations, (2) highlighting polygons of similar orientations to help in stratigraphic reconstructions, (3) linking generalized polygons to the detailed map using GIS capabilities, and (4) compiling separate geologic unit maps and structure maps on a global scale. We look forward to discussion and input from the community on the appropriate directions for the global geologic map of Ganymede.

References. [1] B. Lucchitta, Icarus, 44, 481, 1980; [2] B. Lucchitta and others, USGS Map I-2289, 1992; [3] ACSN, AAPGB, 45, 645, 1961; [4] D. Wilhelms, USGS IP 55, 1972; [5] D. Wilhelms, Cambridge, 208, 1990; [6] J. Head and others, Icarus, 33, 145, 1978; [7] D. Scott and K. Tanaka, USGS Map I-1802A, 1986; K. Tanaka and D. Scott, USGS Map I-1802C, 1987; R. Greeley and J. Guest, USGS Map I-1802B, 1987; [8] E. Shoemaker and others, Sats. of Jupiter, 435, 1982; [9] V. Hansen, EPSL, 176, 527, 2000; [10] G. Collins and others, Icarus, 135, 345, 1998; [11] G. Collins, PhD Thesis, Brown, 2000; [12] G. Collins, LPSC 33, 1783, 2002; [13] M. Golombek and M. Allison, GRL, 8, 1139, 1981; [14] S. Murchie and others, JGR, 91, E222, 1986.

A PROPOSED LUNAR GEOLOGIC MAPPING PROGRAM

Lisa Gaddis, Astrogeology Program, U.S. Geological Survey, Flagstaff, AZ, lgaddis@usgs.gov.

Introduction. A program of support for lunar geologic mapping is proposed by the USGS/Flagstaff. The USGS will define a mapping scheme at local to regional scales and provide digital support data consisting of image and data bases coregistered and projected to uniform scale(s). Lunar scientists will have the opportunity to propose to map regions of the Moon as part of their research programs on the basis of sound science and within the specified scheme. USGS will provide assistance with uniform mapping standards and nomenclature, formal review, and (possibly) creation of USGS I-maps. The purpose of this presentation is to determine the level of interest in the planetary science community for lunar geologic mapping.

Lunar Geologic Mapping. Geologic mapping of the Moon has had a long and varied history, starting with maps compiled from telescopic views in ~1600 by Gilbert and from photographic bases from Luna, Ranger, Zond, and Surveyor missions in the 1950's and 1960's [for example, 1]. The five Lunar Orbiter (LO) missions in 1966 and 1967 provided an excellent photographic image base at ~99% coverage with up to 60-m resolution [2]. Mapping from these data (46 charts) emphasized coverage of candidate Apollo landing sites and included airbrush and orthophotomaps at scales of 1:25,000 and 1:100,000. Forty-four geologic maps at 1:1,000,000 scale were made from these LO data, followed by a 1:5,000,000 near side geologic map [3]. Global geologic mapping coverage was completed with maps of the north, south, east, west, and central far sides [4-8]. A series of large-scale (1:250,000) topographic and orthophotomaps were also made of ~20% of the Moon covered by orbital photography from Apollo 15, 16, and 17 missions.

Controlled global mosaics at ~100 m/pixel resolution and 11 wavelengths from the Clementine mission provide an unparalleled view of the Moon that can support global geologic mapping at scales as large as 1/303 degree/pixel (100 m/pixel). On the basis of these data, we are proposing to support a lunar mapping program that would include geologic and/or thematic maps of local, regional, and global coverage that are identified on the basis of sound science.

Motivation and Mapping Objectives. Research presented at the Lunar and Planetary Science Conference 33 [9-11], Lunar Initiative "New Views of the Moon" meetings [12], and outlined in the report from the NRC Solar System Exploration Committee (Decadal) Review [13] indicate that lunar science is thriving via ongoing analyses of data from Earth-based telescopes, lunar samples, and recent Clementine and Lunar Prospector missions. A common thread among these presentations is preparation for future in situ lunar exploration. Geologic or thematic mapping at high spatial and/or regional resolutions can address several major lunar science questions, including the distribution of major lunar terrain types, the origin of materials (from the crust or mantle) exposed in the South Pole-Aitken basin, the global distribution of ejecta from Imbrium basin, the spatial distribution of permanently shadowed regions (and possibly ice) in the polar regions, and the distribution in space and time of lunar basalts and other volcanic deposits. With the Clementine color data, compositional information can be a significant new component in such lunar geologic and/or thematic maps. Such detailed maps may be required for future mission planning.

Digital Image Bases. For the current systematic geologic mapping programs for Mars and Venus, the USGS provides support for mappers in the form of image and/or digital data bases that have been coregistered and projected to a uniform mapping scale and shape. For the Moon, the fundamental image base for mapping is the controlled Clementine global mosaic of "albedo" at 750-nm [14, 15]. A second

image base that would substantially aid in mapping of near side regions is the digital Lunar Orbiter dataset that is being coregistered to the Clementine 750-nm mosaic [16]. The LO global mosaic is expected to be delivered in September 2003 and will provide low-sun data that is highly complementary to the Clementine color data. These data would be supplemented by global topography and shaded relief data [17]. Additional map bases might include the Clementine UVVIS standard color-ratio data (R=750/415; G=750/950; B=415/750) and similar color-ratio views from the NIR mosaics.

Mapping Schemes. It is currently envisioned that lunar geologic mapping would be performed in digital format in Mercator and Polar Stereographic projections on digital map bases at scales as large as 1/303 (100 m/pixel) or 1/60.6 (500 m/pixel). Both systematic and regional or global mapping schemes are possible. For a systematic lunar mapping program, a 7ºx7º quadrangle mapping scheme based on the 100 m/pixel Clementine data might be appropriate for high-resolution, large-scale mapping (fig. 1). For smaller-scale geologic or thematic mapping, a multiple-quadrangle scheme based on the 500 m/pixel reduced-resolution Clementine data would be more appropriate (fig. 2). Presentation of lunar map products could be as formal as USGS I-maps or as informal as online distribution through the PIGWAD Web site (http://webgis.wr.usgs.gov/).

Comments to the author are invited on any of these topics.

References. [1] Batson and others, 1990, Ch. 2 in Planetary Mapping (Greeley and Batson, eds.). [2] Bowker and Hughes, 1971, Lunar Orbiter Photographic Atlas, NASA SP-206. [3] Wilhelms and McCauley, 1971, Geologic map of the Near Side of the Moon, I-703. [4] Scott and others, 1977, Geologic map of the West Side of the Moon, I-1034; [5] Wilhelms and El-baz, 1977, Geologic map of the East Side of the Moon, I-946; [6] Lucchitta, 1978, Geologic map of the North Side of the Moon, I-1062; [7] Stuart-Alexander, 1978, Geologic map of the Central Far Side of the Moon, I-1047; [8] Wilhelms and others, 1979, Geologic map of the South Side of the Moon, I-1162. [9] Jolliff and others, 2002, LPS XXXIII #1156; [10] Pieters, 2002, LPS XXXIII #1776; [11] Spudis and others, 2002, LPS XXXIII #1104. [12] Jolliff and others, 2000, Eos, Trans. AGU, v. 81, pp. 349. [13] NRC Report, Solar System Exploration, Priorities for 2003 – 2013, July 2002. [14] Eliason and others, 1999, LPS XXX, #1933. [15] Isbell and others, 1997, LPS XXVIII, pp. 623-624. [16] Gaddis and others, 2001, LPX XXXII, #1892. [17] Rosiek and others, 2002, LPS XXXIII, #1792.

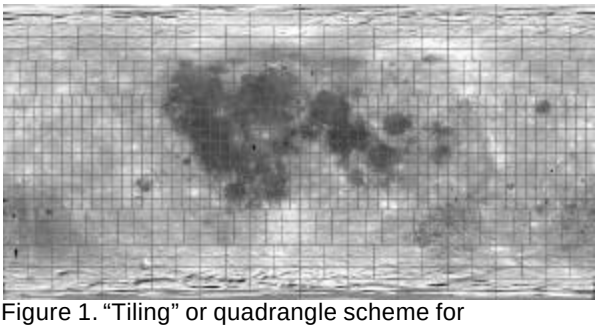

Figure 1. “Tiling” or quadrangle scheme for Clementine UVVIS and NIR global lunar mosaics at 100 m/pixel resolution [14, 15].

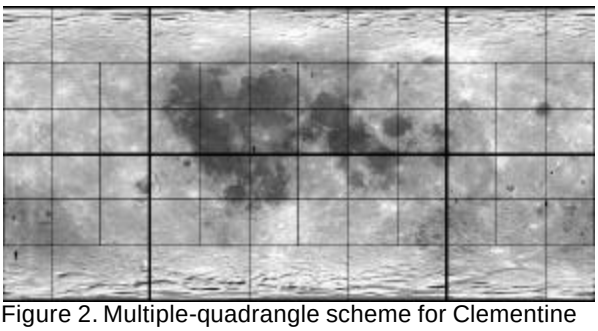

Figure 2. Multiple-quadrangle scheme for Clementine UVVIS and NIR global lunar mosaics at 500 m/pixel resolution [14, 15].